(Masters Thesis)

YASAR UNIVERSITY
GRADUATE SCHOOL OF NATURAL AND APPLIED SCIENCES

SMART ANTENNA SYSTEMS FOR NON-COHERENT SOURCE GROUPS CONTAINING COHERENT SIGNALS

Ahmad AMINU

Thesis Advisor: Asst. Prof. Dr. Mustafa SEÇMEN

Department of Electrical/Electronics Engineering

Presentation Date: 25th June, 2014

Bornova-IZMIR

2014

YASAR UNIVERSITY
GRADUATE SCHOOL OF NATURAL AND APPLIED SCIENCES

SMART ANTENNA SYSTEMS FOR NON-COHERENT SOURCE GROUPS CONTAINING COHERENT SIGNALS

Ahmad AMINU

Thesis Advisor: Asst. Prof. Dr. Mustafa SEÇMEN

Department of Electrical/Electronics Engineering

Presentation Date: 25th June, 2014

Bornova-IZMIR

2014

Approval Page

This study, titled **''Smart Antenna Systems For Non-Coherent Source Groups Containing Coherent Signals''** and presented as Masters thesis by **Ahmad AMINU**, has been evaluated in compliance with the relevant provision of Y.U. Graduate Education and Training Regulations and Y.U. Institute of Science Education and Training. The jury members below have decided for the defence of this thesis, and it has been declared by consensus / majority of votes that the candidate has succeeded in his thesis defence examination dated 25th June, 2014.

Jury Members:	**Signature:**
Head: Asst. Prof. Dr. Mustafa SEÇMEN	**.....**
Rapporteur Member: Asst. Prof. Dr. Nalan OZKURT	**.....**
Member: Asst. Prof. Dr.Ozgur TAMER	**.....**

ABSTRACT

SMART ANTENNA SYSTEMS FOR NON-COHERENT SOURCE GROUPS CONTAINING COHERENT SIGNALS

AMINU, Ahmad

MSc. in Electrical and Electronics Engineering

Supervisor: Asst. Prof. Dr. Mustafa SEÇMEN

June 2014, 88 pages

This study presents smart antenna systems for unknown non-coherent source groups containing coherent signals. All parameters (including the frequency of each signal group) of direction-of-arrival (DOA) problem are aimed to be extracted in the presence of unknown noncoherent source groups, which are consisting of coherent signals. The antenna elements used in the fading analysis and application are isotropic, linear and uniformly distributed, and all parameters of the complete signal are assumed to be unknown except the number of coherent signal in each noncoherent group.

To obtain the desired parameters (number of noncoherent groups, arrival angles, fading coefficients, frequencies), a four-step approach are followed. First, the number of noncoherent signal groups is determined by the minimum description length (MDL). Then, effective steering vectors are estimated using the joint approximate diagonalization of eigenmatrices (JADE) algorithm. In the third step, by using these steering vectors some popular high-resolution DOA methods such as the modified forward backward linear prediction (MFBLP), estimation of signal parameters via rotational invariance techniques (ESPRIT), multiple signal classification (MUSIC), and Minimum-norm (Min-norm) algorithms are realized to calculate the arrival angle and fading coefficient of each coherent signal. Afterwards, a frequency matching is realized to assign the possible frequency to each group.

Root mean square error (RMSE) values for DOAs and fading coefficients are computed in a very challenging case having extreme fading coefficients for all

the methods used and the corresponding results are compared for different scenarios such as different SNR, different number of antenna elements and snapshots. Although all the methods resolved the signals correctly, simulation results show that JADE based MFBLP has the superior performance.

The DOAs obtained from the JADE-MFBLP are then processed using steepest descent, least mean square (LMS) and normalized LMS adaptive beamforming algorithms to steer the main lobe of the radiation pattern to desired angles (signals) and the nulls to undesired angles (signals). The simulation results also reveal that adaptive beamforming is successfully done by cancelling the effects of undesired signals significantly. Finally, the reduction of power in dB for the worst case where all undesired signals are out of phase to the desired signal is investigated. The simulation results present that in spite of challenging environment with strong fading coefficients, the algorithms are able to make a successful beamform adaptively such that the power reduction is observed as 5.80 dB, 1.04dB and 2.86 dB at most for SD, LMS and NLMS respectively.

Keywords: adaptive beamforming, direction of arrival (DOA), estimation of signal parameters via rotational invariance techniques (ESPRIT), fading, joint approximate diagonalization of eigenmatrices (JADE), least mean square (LMS) algorithm, minimum description length (MDL), minimum-norm (Min-norm), modified forward backward linear prediction (MFBL), multiple signal classification (MUSIC)

ÖZET

Bu çalışma, uyumlu sinyaller içeren bilinmeyen uyumlu olmayan kaynak grupları için akıllı anten sistemlerini sunmaktadır. Geliş yönü probleminin tüm parametreleri (her sinyal grubunun frekansını içeren) uyumlu sinyallerden oluşan bilinmeyen uyumlu olmayan kaynak grupları varlığında ayıklanması amaçlanmıştır. Sönümleme analizinde kullanılan anten elemanları izotropiktir, doğrusal ve düzgün dağılımlıdır ve sinyalin tüm parametreleri her uyumlu olmayan gruptaki uyumlu sinyal sayısı dışında bilinmiyor varsayılmıştır.

İstenilen parametreleri (uyumlu olmayan grup sayısı, geliş açısı, zayıflama katsayıları, frekanslar) elde etmek için dört aşamalı yaklaşım izlenmiştir. İlk olarak, uyumlu olmayan sinyal gruplarının sayısı minimum tanımlama uzunluğu ile belirlenmiştir. Sonra, öz ortak yaklaşık köşegenleştirme algoritması kullanılarak etkili yönelimvektörleri kestirilmiştir. Üçüncü aşamada ise bu yönelim vektörleri; modifiye edilmiş ileri geri lineer tahmin (MFBLP), rotasyonel değişmezlik tekniği ile sinyal parametrelerinin kestirimi (ESPRIT), çoklu sinyal sınıflandırma (MUSIC), temel çoklu sinyal sınıflandırma (root-MUSIC) ve minimum norm (Min-norm) algoritmaları gibi bazı yüksek çözünürlükte DOA metodları kullanılarak açı ve her uyumlu sinyalin zayıflama katsayısının hesaplama işlemi gerçekleştirilmiştir. Ardından her gruba frekans atamak için frekans eşleştirme yapılmıştır.

Her metod kullanılarak DOA'lar için ortalama hata kareleri toplamı kökü (RMSE) ve zayıflama katsayıları için bağıl RMSE değerleri farklı senaryolarda hesaplandı ve karşılaştırma yapıldı. Tüm metodlar sinyali doğru çözümlemesine rağmen simülasyon sonuçları JADE tabanlı MFBLP yönetmin en iyi performansa sahip olduğunu gösterdi.

Jade-MFBLP'den elde edilen DOA'lar, radyasyon paterninin ana lobunu istenilen açıya yönlendirmek için ve istenmeyen açılarda sıfıra denk gelmesi içindik iniş, en küçük karesel ortalama (LMS) ve normalize LMS adaptif hüzme şekillendirme algoritmaları kullanılarak işleme konuldu. Simülasyon sonuçları, adaptif hüzme şekillendirici yönteminin istenmeyen sinyal etkilerini yok etmede başarılı olduğunu gösterdi. Son olarak, tüm istenmeyen sinyallerin istenen sinyale göre faz dışında kalması en kötü durum olarak kabul edildi ve bu durumda sinyaldeki düşüş dB cinsinden incelendi. Simülasyon sonuçları, güçlü zayıflama katsayılı zorlu çevre şartlarına rağmen, algoritmaların adaptif olarak başarılı hüzme yapabildiğini gösterdi. Örneğin M=12 ve M=500 enstantenesinde LMS,

NLMS ve dik iniş algoritmaları ile alınan güç azalma sonuçları sırasıyla 1.04 dB, 2.86dB ve 5.80dB olduğu gözlemlendi.

Anahtar Kelimeler: adaptif hüzme şekillendirme, varış açısı, rotasyonel değişmezlik tekniği yöntemiyle sinyal parametrelerinin kestirimi, zayıflama, özmatrislerin birleşik yakın köşegenleştirilmesi, en küçük karesel ortamala algoritması, minimum tanımlayıcı uzunluk, minimum norm, modifiye edilmiş ileri geri lineer tahmin, çoklu sinyal sınıflandırma, normalize en küçük karesel ortalama algoritması, temel çoklu sinyal sınıflandırma

ACKNOWLEDGEMENTS

First, I would like to thank Allah subhaanahuu wa ta'ala for the knowledge and strength that made this research work possible. I would like also to thank my supervisor Asst. Prof. Dr. Mustafa Seçmen for his tireless contribution, guidance and patience during this study. In addition, I would like to thank the jury members and also staff of Electrical and Electronics Engineering department, Yasar University, for their support and encouragement towards the successful completion of this thesis and indeed the MSc program.

I would also like to express my sincere gratitude to my wife especially for her patience and encouragement, my children, rest of the family and friends here in Turkey and also those in Nigeria for their well wishes. I thank you very much.

Finally, my profound gratitude goes to His Excellency, the executive governor of Kano state, Engr. (Dr.) Rabi'u Musa Kwankwaso and his cabinet for the scholarship awarded to me to undergo this postgraduate program here at Yasar University, Izmir Turkey.

AMINU, Ahmad

TEXT OF OATH

I declare and honestly confirm that my study, titled **''Smart Antenna Systems For Non-Coherent Source Groups Containing Coherent Signals''** and presented as a Master's thesis, has been written without applying to any assistance inconsistence with scientific ethics and traditions, that all sources from which I have benefited are listed in the bibliography, and that I have benefited from these sources by means of making references.

Date: 25th June, 2014

Ahmad AMINU

Signature:.....

TABLE OF CONTENT

Pages

INDEX OF FIGURE

INDEX OF TABLE

1. INTRODUCTION

1.1 Background of the Study

Wireless Communication is growing with a very rapid rate for several years. The progress in radio technology enables new and improved services. Current wireless services include transmission of voice, fax and low-speed data. More bandwidth consuming interactive multimedia services like video-on demand and internet access are supported.

Wireless systems that enable higher data rates and higher capacities have become the need of the present time (Khumane et al., 2011). At the same time, operators want to support more users per base station in order to reduce overall network cost and make the services affordable to subscribers. Wireless networks must provide these services in a wide range of environments, dense urban, suburban, and rural areas. Because the available broadcast spectrum is limited, attempts to increase traffic within a fixed bandwidth create more interference in the system and degrade the signal quality (Tsoulos, 1999).

The solution to this problem is “SMART ANTENNA”. Today's modern wireless mobile communications depend on adaptive "smart" antennas to provide maximum range and clarity. With the recent explosive growth of wireless applications, smart antenna technology has achieved widespread commercial and military applications (Tsoulos et al., 1995)

Any smart antenna system merges an antenna array and a signal processing unit to combine the incident signals on the array adaptively through weight adjustment. The signal processing consists of direction of arrival (DOA) estimation and adaptive beamforming part. Various methods for DOA estimation and beamforming are available, which differ in accuracy, computational complexity and convergence speed. The appropriate algorithm for DOA estimation or beamforming may differ from one application to another. DOA estimation is an important problem in array signal processing. Angle estimation may be used for source localization or source tracking by determining the desired signal location or may be exploited to reduce the unwanted effects of noise and interference. Therefore, DOA estimation, Angle of Arrival (AOA) or Time of Arrival (TOA) estimation is applicable in various fields such as radar, sonar, navigation, geophysics, wireless communications and so on (Balanis, 2005),

(Chen et al., 2010). In adaptive array antennas or smart antenna systems, DOA estimation algorithms provide information about the system environment for an efficient beamforming or providing location-based services such as emergency services. Therefore, great researches have been accomplished about DOA estimation during recent years, including different methods, different signal and system conditions, different array geometries and applications (Okamoto, 2002), (Balanis, 2005).

The studies described above and traditional theory of DOA estimation are based on the sources (or signals) which are uncorrelated (noncoherent) to each other. These noncoherent signals can be considered as multiple users or frequencies in the wireless communication applications. The estimation of DOA angles for these types of signals are relatively easier and classical DOA estimation can be safely applied for this purpose. Then, the beamforming algorithms can be carried out to get maximum signal from one user and minimum signals from other users which can be treated as interference signals. However, since the frequencies of different users are different due to noncoherent behaviours of the signals, the effective cancellation of undesired signals (users) can be realized by putting suitable narrow passband filters even beamforming techniques are not used. On the other hand, more difficult and challenging scenario is observed when the desired and undesired signals are coherent (correlated) such as multipath signals. Multipath or fading signals are time-shifted replicas of the original desired signals (usually coming from different incident angles than that of original desired signal); so their frequencies are same as the desired signals. Therefore, they could not be annihilated by using filter approach. These multipath signals have very adverse effects such as total cancellation of the desired signal. Therefore, the reducing the effect of multipath signals of the same user is much more important than the decreasing the signal levels of other users (different frequencies). The difficulty in DOA estimation under multipath propagation is that since the desired and undesired fading signals are coherent, the classical DOA estimation algorithms cannot be directly used, and more intelligent methods should be used.

With these intelligent methods, smart antennas combining DOA estimation under coherent signal environment and corresponding beamforming can improve the system performance by helping the channel modelling and suppression undesirable signals like multipath fading and co-channel interference (Varade et al., 2009).

1.2 Scope of the Thesis

By regarding to the difficulties explained above for the smart antenna systems for signals with multipath effect, the scope of this thesis is limited to simulation of different DOA and fading coefficients estimation algorithms in multipath propagation, frequency matching and adaptive beamforming with a view to implement smart antenna system for wireless and mobile communication systems. For this purpose, several DOA estimation algorithms such as ESPRIT, MUSIC, root-MUSIC Min-norm and MFBLP in conjunction with JADE are realized to estimate the DOAs of different coherent signals (multipath environment) and then steepest descent, LMS and NLMS beamforming algorithms are used to adjust the complex weights and to generate an optimized radiation pattern with mainlobes and nulls in the direction of desired and undesired signals, respectively.

1.3 Aim of the Study

This study aimed at implementing Smart Antenna System especially for high frequency and non-coherent source groups each having coherent signals. The excitation coefficients of the antenna array elements are going to be optimized to maximize the main lobes toward the signal-of-interest (SOI) angles and nulls toward the signal-not-of-interest (SNOI) angles. For this purpose several direction-of-arrival algorithms and beam forming algorithms are realized to obtain a sufficient method even under noisy signal conditions. The study also aimed at estimating and correctly matching different frequencies to different non-coherent source groups and this will be the main contribution of this thesis to the literature of direction of arrival (DOA) estimation.

1.4 Methodology of the Study

In the first stage of the thesis, minimum description length (MDL) is used to determine the number of non-coherent source groups and then, joint approximate diagonalization of eigenmatrices (JADE) algorithm is used to estimate the generalized steering vectors.DOA parameters such as angles of arrival and fading coefficients are estimated by using several high resolution methods such as ESPRIT, MUSIC, ROOT-MUSIC, MFBLP and Min-norm and their results are compared. Frequency matching to non-coherent signal groups is also done in this stage.

The second stage involves using steepest descent, LMS and normalized LMS algorithms for beam forming to steer the main lobes of the array toward the signals-of interest (SOI) and nulls to the signals-not-of-interest (SNOI).

1.5 Thesis Outline

The report of the thesis is outline as follows. Chapter 2 contains the background knowledge of antenna and antenna systems, types of antenna, smart antenna systems and its types, advantages and disadvantages.

In chapter 3, the signal model, DOAs and fading coefficients estimation algorithms are discussed. The concept of frequency or group matching is also introduced in this chapter.

Chapter 4 includes the simulation results for DOA and fading coefficients, frequency/group matching result as well as comparative analysis results of different types of DOA and fading coefficients estimation algorithms.

The adaptive beamforming algorithms such as steepest descent, least mean square (LMS) and normalized LMS are discussed in chapter 5.

Chapter 6 discusses the simulation results of steepest descent, LMS and NLMS, in addition to the effect of changing the number of antenna elements and spacing between elements on the beamforming and on the mean square error. Finally, the effect of step-size on the beamforming and on the convergence speed of the two beamforming algorithms was investigated also in this chapter.

Conclusions and suggestion for future works are given in chapter 7.

2. THE OVERVIEW OF SMART ANTENNA SYSTEMS

In this chapter, the concept of antenna, direction of arrival and smart antenna systems are presented to give an insight and better understanding of the contents of the thesis.

2.1 Antenna

An antenna (or aerial) is a transducer designed to transmit or receive electromagnetic waves. In other words, antennas convert electromagnetic waves into electrical currents and vice versa. Antennas are used in systems such as radio and television broadcasting, point-to-point radio communication, wireless LAN, radar, and space exploration. Antennas are most commonly employed in air or outer space, but can also be operated under water or even through soil and rock at certain frequencies for short distances (Okamoto, 2006).

Physically, an antenna is simply an arrangement of one or more conductors, usually called *elements*. In transmission, an alternating current is created in the elements by applying a voltage at the antenna terminals, causing the elements to radiate an electromagnetic field. In reception, the inverse occurs such that an electromagnetic field from another source induces an alternating current in the elements and a corresponding voltage at the antenna's terminals. Some receiving antennas (such as parabolic types) incorporate shaped reflective surfaces to collect EM waves from free space and direct or focus them onto the actual conductive elements.

There are two fundamental types of antenna directional patterns, which, with reference to a specific three dimensional (usually horizontal or vertical) plane are either:

- Omni-directional (radiates equally in all directions), such as a vertical rod.
- Directional (radiates more in one direction than in the other).

2.1.1 Omni directional Antenna

Omni-directional usually refers to all horizontal directions with reception above and below the antenna being reduced in favour of better reception (and thus range) near the horizon.

Since the early days of wireless communications, there has been the simple dipole antenna, which radiates and receives equally well in all directions. To find its users, this single-element design broadcasts omnidirectionally in a pattern resembling ripples radiating outward in a pool of water as shown in Fig. 2.1 below. While adequate for simple RF environments where no specific knowledge of the users' whereabouts is available, this unfocused approach scatters signals, reaching desired users with only a small percentage of the overall energy sent out into the environment.

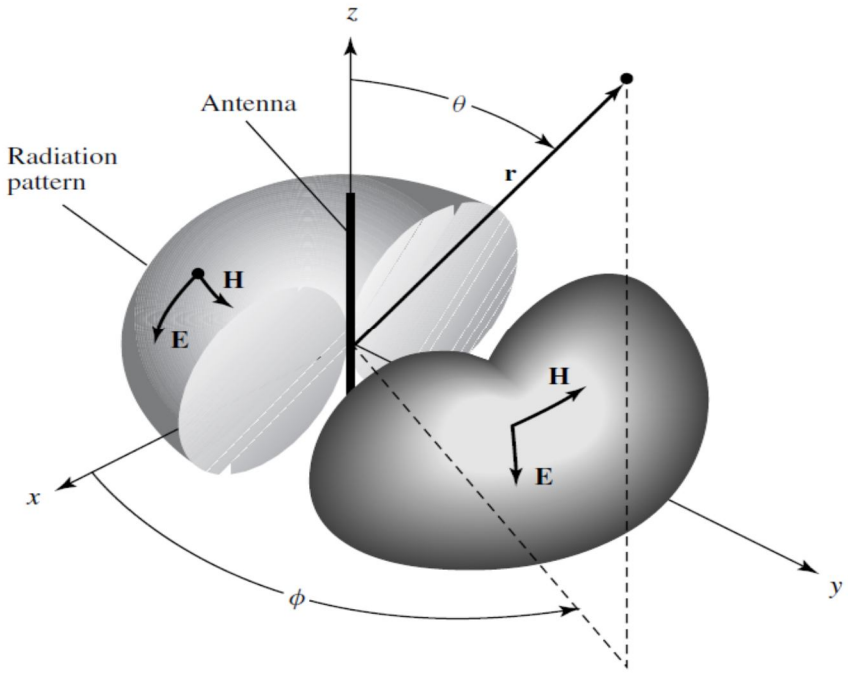

Figure 2.1: Omni-directional Antenna pattern (Balanis, 2005)

With this limitation, omnidirectional strategies attempt to overcome environmental challenges by simply boosting the power level of the signals broadcast. In a setting of numerous users (and interferers), this makes a bad situation worse in that the signals that miss the intended user become interference for those in the same or adjoining cells.

In uplink applications (user to base station), Omni directional antennas offer no preferential gain for the signals of served users. In other words, users have to shout over competing signal energy. Also, this single-element approach cannot selectively reject signals interfering with those of served users and has no spatial multipath mitigation or equalization capabilities.

Omni directional strategies directly and adversely impact spectral efficiency, limiting frequency reuse. These limitations force system designers and network planners to devise increasingly sophisticated and costly remedies. In recent years, the limitations of broadcast antenna technology on the quality, capacity, and coverage of wireless systems have prompted an evolution in the fundamental design and role of the antenna in a wireless system.

2.1.2 Directional Antenna

A "directional" antenna usually refers to one focusing a narrow beam in a single specific direction as shown in Fig. 2.2 below. A single antenna can also be constructed to have certain fixed preferential transmission and reception directions. As an alternative to the brute force method of adding new transmitter sites, many conventional antenna towers today split, or sectorized cells. A 360° area is often split into three 120° subdivisions, each of which is covered by a slightly less broadcast method of transmission.

All else being equal, sector antennas provide increased gain over a restricted range of azimuths as compared to an omnidirectional antenna. This is commonly referred to as antenna element gain and should not be confused with the processing gains associated with smart antenna systems.

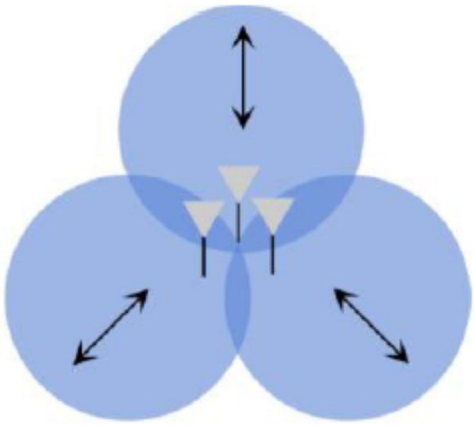

Figure 2.2: Directional Antenna Pattern (Jain, 2011)

While sectorized antennas multiply the use of channels, they do not overcome the major disadvantages of standard omnidirectional antenna broadcast such as co-channel interference.

All antennas radiate some energy in all directions in free space but careful construction results in substantial transmission of energy in a preferred direction and negligible energy radiated in other directions.

Smart antenna systems normally use more than one antenna elements; consequently, even if the antenna elements are omnidirectional, the overall array structure is directional. The main aim of the smart antenna systems is to direct the mainbeam of the radiation pattern of the array towards the desired signal and put nulls at the angles of undesired ones in the radiation pattern. The traditional phased antenna array technology (Balanis, 2005) can direct the main beam of the radiation pattern of the array to the desired signal's angle of arrival once DOA angle of the desired signal is estimated. However, it does not care about the positioning of nulls at the undesired signals' DOA angles. Therefore, it is not evaluated as a smart antenna system. On the other hand, some null insertion antenna methods such as Schelkunoff polynomial method (Balanis, 2005) can successfully put nulls at the DOA angles of undesired signals in the radiation pattern. Nevertheless, they have no abilities to maximize the level of desired signal such that the main beam of the array is usually not directed to the DOA of desired angle, and even DOA of desired signal may corresponds to the null in the pattern.

2.2 Smart Antennas

The smart antenna systems can be understood better when its working principles are compared with human body (Balanis, 2005). Figure 2.3 below depicts the human analogy as well as the electrical equivalent of smart antenna systems.

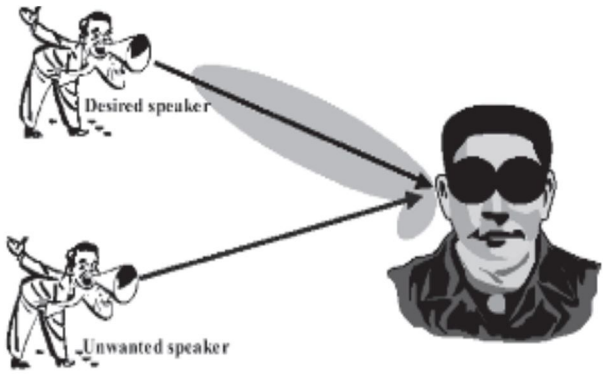

(a) Human analogy

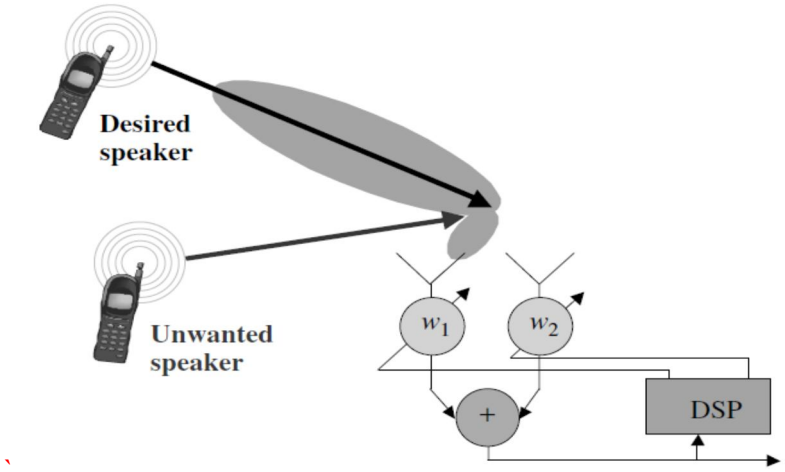

(b) Electrical equivalent

Figure 2.3 Smart Antenna Analogy (a) Human analogy (Balanis, 2005); (b) Electrical equivalent

Therefore, to give an insight into how a smart-antenna system works, let us imagine two persons carrying on a conversation inside a dark room (Balanis, 2005) [refer to Figure 2.3(a)]. The listener among the two persons is capable of determining the location of the speaker as he moves about the room because the voice of the speaker arrives at each acoustic sensor, the ear, at a different time. The human signal processor, the brain, computes the direction of the speaker from the time differences or delays of the voice received by the two ears. Afterward, the brain adds the strength of the signals from each ear so as to focus on the sound of the computed direction. Furthermore, if additional speakers join in the conversation, the brain can tune out unwanted interferers and concentrate on one conversation at a time (Balanis, 2005). Conversely, the listener can respond back to the same direction of the desired speaker by orienting the transmitter (mouth) toward the speaker.

Electrical smart-antenna systems work the same way using two antennas instead of the two ears and a digital signal processor instead of a brain(Balanis, 2005) [refer to Figure 2.3(b)]. Therefore, after the digital signal processor measures the time delays from each antenna element, it computes the direction of arrival (DOA) of the signal-of-interest (SOI), and then it adjusts the excitations (gains and phases of the signals) to produce a radiation pattern that focuses on the SOI while, ideally, tuning out any signal-not-of interest (SNOI) (Balanis, 2005).

Contrary to the name smart antennas consist of more than an antenna. A smart antenna is an antenna system, which dynamically reacts to its environment to provide better signals and frequency usage for wireless communications. There are a variety of smart antennas which utilize different methods to provide improvements in various wireless applications.

The concept of using multiple antennas and innovative signal processing to serve cells more intelligently has existed for many years. In fact, varying degrees of relatively costly smart antenna systems have already been applied in defence systems. Until recent years, cost barriers have prevented their use in commercial systems (Balanis, 2005). The advent of powerful low-cost digital signal processors (DSPs) and general-purpose processors, as well as innovative software-based signal-processing techniques (algorithms) have made intelligent antennas practical for cellular communications systems (Balanis, 2005).

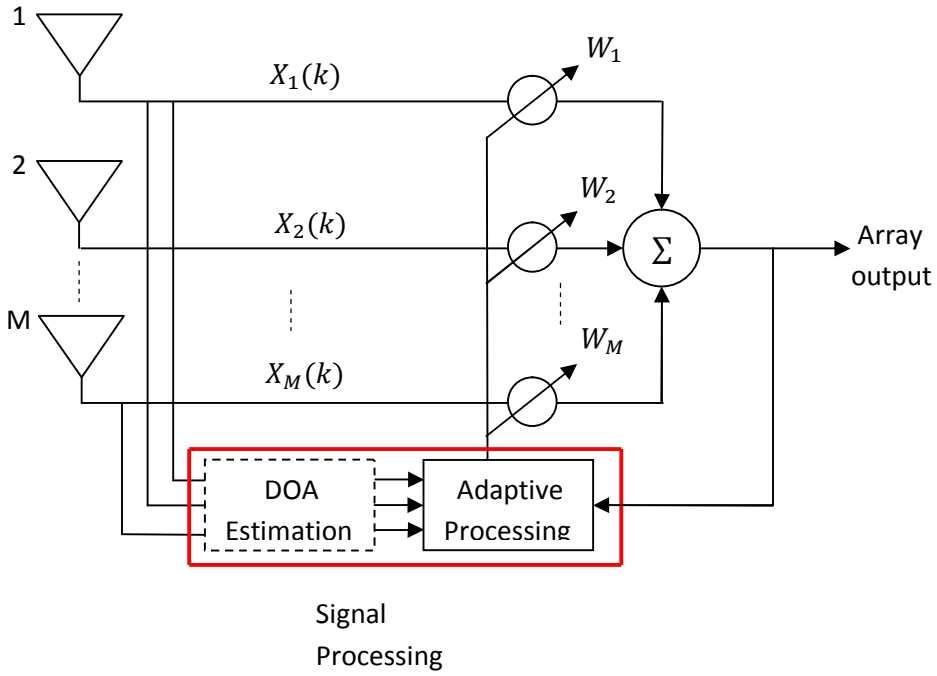

Figure 2.4: A Sample Smart Antenna System (Moghaddam, 2012)

Today, when spectrally efficient solutions are increasingly a business imperative, these systems are providing greater coverage area for each cell site, higher rejection of interference, and substantial capacity improvements. Figure 2.4 above shows the general block diagram of a sample smart antenna system.

2.3 Types of Smart Antenna

The two major categories of smart antennas regarding the choices in transmit strategy are Adaptive and Switch beam.

2.3.1 Adaptive Array

Adaptive antennas which consist of an infinite number of patterns (scenario-based) that are adjusted in real time represents the most advanced smart antenna approach to date (Tsoulos et al., 1995).Using variety of available signal processing algorithms, the adaptive system takes advantage of its ability to effectively locate and track various types of signals to dynamically minimize interference and maximize intended signal reception as shown in Figure2.5 below.

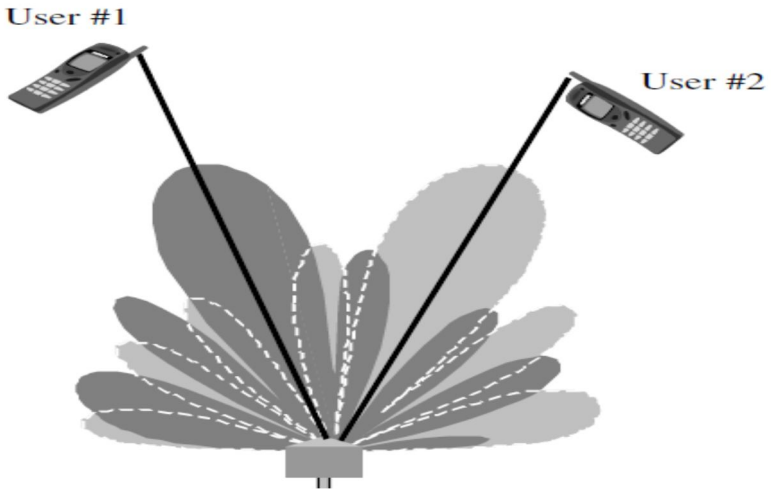

Figure 2.5: Adaptive Array System, Representative Depiction of a Main Lobes Extending Toward desired Users (Balanis, 2005)

2.3.2 Switched Beam

Switched beam antenna systems which consist of finite number of fixed, predefined patterns or combining strategies (sectors) form multiple fixed beams as shown in Figure 2.6 below, with heightened sensitivity in a particular direction. These antenna systems detect signal strength, choose from one of several predetermined, fixed beams, and switch from one beam to another as the mobile moves throughout the sector (Khumane et al., 2011).

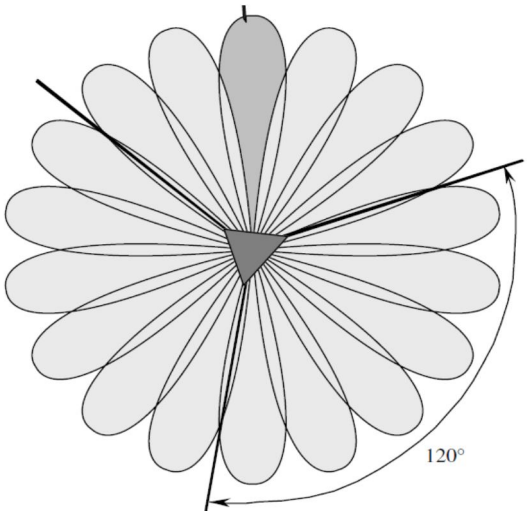

Figure 2.6: Switched beam system (Balanis, 2005)

Instead of shaping the directional antenna pattern with the metallic properties and physical design of a single element (like a sectorized antenna), switched beam systems combine the outputs of multiple antennas in such a way as to form finely sectorized (directional) beams with more spatial selectivity than can be achieved with conventional approaches.

The task of transmitting in a spatially selective manner is the major basis for differentiating between switched beam and adaptive array systems. As described above, switched beam systems communicate with users by changing between preset directional patterns, largely on the basis of signal strength. In comparison, adaptive arrays attempt to understand the RF environment more comprehensively and transmit more selectively. Both systems attempt to increase gain according to the location of the user, however, only the adaptive system provides optimal gain while simultaneously identifying, tracking, and minimizing interfering signals.

2.4 WorkingPrinciples of Smart AntennaSystems

Adaptive array and switched beam systems enable a base station to customize the beams they generate for each remote user effectively by means of internal feedback control. Generally speaking, each of the two approaches forms a main lobe toward individual users and attempts to reject interference or noise from outside of the main lobe.

2.4.1 Listening to the Cell (Uplink Processing)

It is assumed here that a smart antenna is only employed at the base station and not at the handset or subscriber unit. Such remote radio terminals transmit using omnidirectional antennas, leaving it to the base station to separate the desired signals from interference selectively. Typically, the received signal from the spatially distributed antenna elements is multiplied by a weight, a complex adjustment of amplitude and a phase. These signals are combined to yield the array output. An adaptive algorithm controls the weights according to predefined objectives. For a switched beam system, this may be primarily maximum gain; for an adaptive array system, other factors may receive equal consideration. These dynamic calculations enable the system to change its radiation pattern for optimized signal reception.

2.4.2 Speaking to the Users (Downlink Processing)

The type of downlink processing used depends on whether the communication system uses time division duplex (TDD), which transmits and receives on the same frequency (e.g., PHS and DECT) or frequency division duplex (FDD), which uses separate frequencies for transmit and receiving (e.g., GSM). In most FDD systems, the uplink and downlink fading and other propagation characteristics may be considered independent, whereas in TDD systems the uplink and downlink channels can be considered reciprocal. Hence, in TDD systems uplink channel information may be used to achieve spatially selective transmission. In FDD systems, the uplink channel information cannot be used directly and other types of downlink processing must be considered.

2.5 Advantages and Disadvantages of Smart Antennas

2.5.1 Advantages

- Increased Number of Users

Due to the targeted nature of smart antennas, frequencies can be reused allowing an increased number of users. More users on the same frequency space means that the network provider has lower operating costs in terms of purchasing frequency space.

- Increased Range

As the smart antenna focuses gain on the communicating device, the range of operation increases. This allows the area serviced by a smart antenna to increase. This can provide a cost saving to network providers as they will not require as many antennas/base stations to provide coverage.

- Geographic Information

As smart antennas use 'targeted' signals the direction in which the antenna is transmitting and the gain required to communicate with a device can be used to determine the location of a device relatively accurately. This allows network providers to offer new services to devices. Some services include, guiding emergency services to locations, location based games and locality information.

- Security

Smart antennas naturally provide increased security, as the signals are not radiated in all directions as in a traditional omni-directional antenna. This means that if someone wished to intercept transmissions they would need to be at the same location or between the two communicating devices.

- Reduced Interference

Interference which is usually caused by transmissions which radiate in all directions is less likely to occur due to the directionality introduced by the smart antenna. This aids both the ability to reuse frequencies and achieve greater range.

- Increased bandwidth

The bandwidth available increases form the reuse of frequencies and also in adaptive arrays as they can utilize the many paths which a signal may follow to reach a device.

2.5.2 Disadvantages

- Complex

One of the disadvantages of smart antennas is that, they are far more complicated than traditional antennas. This means that faults or problems are more likely to occur and harder to be diagnosed.

- More Expensive

As smart antennas are extremely complex, utilizing the latest in processing technology they are far more expensive than traditional antennas. However, this cost must be weighed against the cost of frequency space.

- Larger Size

Due to the antenna arrays which are utilized by smart antenna systems, they are much larger in size than traditional systems. This can be a problem in a social context as antennas can be seen as ugly or unsightly.

3. SIGNAL MODEL AND THE STEPS OF PROPOSED METHOD FOR DOA ESTIMATION

In this chapter, the data model for the overall signal on the antenna elements and problem geometry will be given. The steps of the DOA estimation part of the study are discussed in detail by including DOA estimation algorithms, fading coefficients estimation and frequency matching for noncoherent source groups containing coherent signals. The similar methods in literature, which use same signal model, are also described in the chapter, and their drawbacks are going to be explained.

3.1 Array Model for Noncoherent Source Groups Containing Coherent Signals

In the array model of the problem, it is assumed that there are N narrowband signals arriving to the array in the directions $\{\theta_1, \theta_2, \theta_3, \ldots, \theta_N\}$. In order to simplify the problem under consideration, a uniform linear array (ULA) shown in Figure 3.1 below is assumed with inter-element spacing d of half wavelength of the narrowband signal frequency. In the mentioned figure, only one plane wave being incident in the direction θ is depicted for simplicity such that total of N plane waves actually exists in the system. M antenna elements in the array of Figure 3.1 have identical isotropic responses, and "the reference point" of the system is taken as the leftmost antenna element in the array.

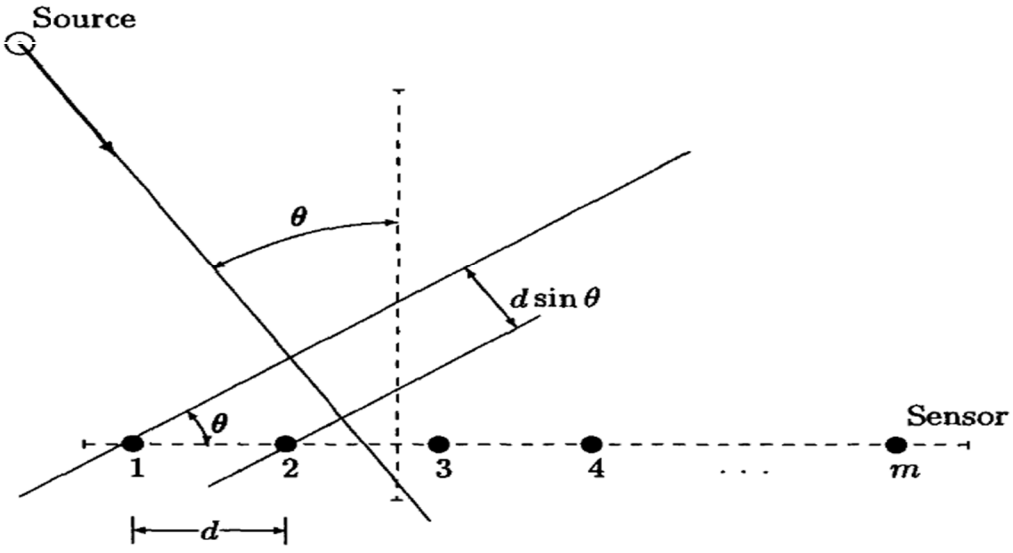

Figure 3.1: Uniform Linear Array with M Antenna Elements Where a Sample Plane Wave Impinges upon the Array at the Direction of Arrival of θ.

In the model, K different RF or down converted IF frequencies $\{\omega_1, \omega_2,\ldots,\omega_K\}$ are used to denote the number of different users in wireless communication. At each frequency (group), there are L coherent signals (assumed to be known) where $K\times L$ is equal to N. All parameters of the complete signal are assumed to be unknown except the number of coherent signal in each noncoherent group.

Data received at antenna elements can be described by an $M \times 1$ vector as:

$$\mathbf{X}(k) = \mathbf{A}\mathbf{s}(k) + \mathbf{n}(k) \qquad k = 1,...,N_s \tag{3.1}$$

where N_s is the number of snapshots and **A** is the array steering matrix which is described for uniform linear array as:

$$\mathbf{A} = \left[a(\theta_1) \quad a(\theta_2) \quad \cdots \quad a(\theta_N) \right] \tag{3.2}$$

$$a(\theta_n) = [1 \quad e^{j2\pi d \sin\theta_n/\lambda} \quad \cdots \quad e^{j2\pi d(M-1)\sin\theta_n/\lambda}]^T \tag{3.3}$$

where d and λ are antenna inter-element spacing and signal wavelength, respectively. In equation (3.1), **s** is a vector of signals including the fading coefficients of the signals such that

$$\mathbf{s}(k) = \left[\rho_1 e^{j\omega_1 k} \quad \rho_2 e^{j\omega_1 k} \quad \cdots \quad \rho_L e^{j\omega_1 k} \quad \cdots \quad \rho_N e^{j\omega_K k} \right]^T \tag{3.4}$$

where$\rho_1,\ldots,\rho_N$ are complex fading coefficients of the signals. Here, the signals and correspondent fading coefficients from $n = 1,\ldots,L$ belongs to first group (frequency), and the fading coefficients from $n = N\text{-}L\text{+}1,\ldots, N$ belongs to signals in last group. The **n** in (3.1) is a vector of additive white Gaussian noise. It is assumed that the entries of $\mathbf{s}(k)$ and $\mathbf{n}(k)$ are zero mean processes and the entries of $\mathbf{n}(k)$ are independent with each other and signals.

Researchers in the area of signal processing have been working for decades to try to resolve highly correlated signals, which are resulted due to multipath and fading phenomena as described above. Coherent signals cause covariance matrix to be singular with rank loss and zero determinant which means the signals cannot be directly resolved using second order statistics base subspace methods. Several other techniques were developed to take care of coherency problems such as maximum likelihood (Stoica et al., 1996), spatial smoothing (Pillai, 1989) and matrix pencil (MP) (Yilmazer et al., 2006). Maximum likelihood is computationally intensive, spatial smoothing requires more sensors for pre-processing and matrix pencil (MP) requires high signal to noise ratio (SNR). Other methods include fourth order cumulants (FOC) such as steering vectors DOA (Yuen et al., 1997) which first estimates the steering vectors and then it utilizes MFBLP to estimates DOA using the estimated vectors. This method requires large number of snapshots. At present, JADE algorithm (Cardoso et al., 1993) has been successfully applied to DOA applications that it allows estimating the array response vectors without having a prior knowledge of the array manifold.

Although all the methods/algorithms above are somehow successful in the estimation of arrival angles and fading coefficients even under the case of noncoherent source groups each including superposition of coherent signals, they do not care about the frequency estimation of the signals. In other words, the frequency matching (which frequency belongs to which signal group) is not considered by these methods. However, the frequency matching is crucial in multi-user applications such as mobile communication where each frequency can be assigned to a user. The multi-beam generated by the antenna elements can be considered as the beamforming for each signal group (each frequency) in smart antenna systems. Therefore, even the proper excitation coefficients for the antenna elements are determined for each group, the corresponding carrier (or IF) frequency should be also found, and it can be done only with a proper frequency matching.

In the next section the steps of the proposed method are going to be explained in detail.

3.2 Minimum Description Length (MDL) Algorithm

In the first step, the number of noncoherent signal groups, in other words, number of frequencies (*K*), is determined by using minimum description length (MDL) under the additive white Gaussian noise. MDL is a classical method (Wax et al., 1985), which uses the covariance matrix of **X**(*k*) in (3.1) and minimizes the function (3.6) by using the eigenvalues of this covariance matrix. MDL criterion is summarized in two steps (Wax et al., 1985) as follows:

- Form the array covariance matrix

$$R = E\{\boldsymbol{X}(t)\boldsymbol{X}^H(t)\} \tag{3.4}$$

The number of groups is determined as the value of $k \in \{0,1,2 \dots M\}$that MDL is minimized.

$$MDL = -(M-k)N_s \log\left(\frac{\prod_{i=k+1}^{M}\lambda_i^{\frac{1}{M-k}}}{\frac{1}{M-k}\sum_{i=k+1}^{M}\lambda_i}\right) + \frac{1}{2}(2M-k)logN_s \tag{3.6}$$

where $\lambda_1 > \lambda_2 > \lambda_3 \dots > \lambda_M$ are eigenvalues of the covariance matrix.

3.3 Steering Vector Estimation Using JADE Algorithm

In the second step of the proposed method, JADE algorithm is realized to get the generalized steering vectors (Cardoso et al., 1993). There are *K* steering vectors, whose number of elements is equal to that of antenna elements (*M*). These vectors include the arrival angle and fading coefficient information. It is summarized as follows (Tufts et al., 1982).

- Compute whitening matrix ***W***. Whitening process can be expressed as

$$Z = WX(t) \tag{3.7}$$

- Form fourth order cumulants of $Z(t)$

- Jointly diagonalize the set $\{\lambda_{Zr}, M_{Zr}, r = 1,2,3,\dots K\}$ by a unitary matrix U that eigenpairs $\{\lambda_{Zr}, M_{Zr}\}$ corresponds to the *K* largest eigenvalues.

- Estimate the array response matrix

$$A = W^{\dagger} U \tag{3.8}$$

Where $W^{\dagger}$ is Moore-Penrose inverse of whitening matrix.

3.4 DOA Estimation Algorithms

In the third step of the method, after K many steering vectors are collected, each vector is processed with a selected high-resolution DOA estimation technique to extract the DOA angles of each group. However, most of these techniques are parametric methods, which need to the number of coherent signals in each group (L) assumed to be known in the analysis and simulations.

These high-resolution DOA estimation algorithms include, multiple signal classification (MUSIC), root-MUSIC, Minimum norm, estimation of signal parameters via rotational invariance technique (ESPRIT) and modified forward backward linear prediction (MFBLP).

3.4.1 MUltiple SIgnal Classification (MUSIC) Algorithm

Multiple signal classification (MUSIC) was developed by Schmidt (Schmidt, 1986). In this method, the spatial covariance matrix is decomposed into signal and noise subspace and then the expression in (3.9) search all the available steering vectors and determine those that are orthogonal to the noise subspace. The output power spectrum of MUSIC is defined in (3.9) below as (Nwalozie et al., 2013):

$$P_{MUSIC}(\theta) = \frac{1}{a^{H}(\theta) Q_n Q_n^{H} a(\theta)} \tag{3.9}$$

Where Q_n is the noise subspace and $(.)^{H}$ is the conjugate transpose. From (3.9) if θ corresponds to one of the DOAs then $a(\theta) \perp Q_n$ and the denominator becomes identically zero, therefore, the output will have peak value, hence the direction of arrival.

3.4.2 Minimum norm Algorithm

This method was proposed by kumaresan and Tufts (Kumaresan et al., 1983) and it is applicable to linear arrays. The general expression for this method is to search for the locations of the peaks in the spectrum:

$$P_{Min-norm} = \frac{1}{\left| a^H(\theta) Q_n Q_n^H Y Q_n Q_n^H a(\theta) \right|} \tag{3.10}$$

where $Y = pp^T$ and p is the first column of M x M identity matrix. Y is used in the expression to ensure that the matrix dimensions match. Min-norm could be regarded as improvement to MUSIC since the denominator of the expression looks like the square of that of MUSIC, hence all values near zero serve to boost the power output to a higher level.

3.4.3 Root-MUSIC Algorithm

Root-MUSIC algorithm for DOA estimation which was proposed by Barabell (Barabell, 1983) and can only be used for linear arrays. The method performs better than spectral MUSIC especially at low signal to noise ratio (Barabell, 1983) and it involves expressing the array steering vectors in polynomial form by evaluating at $z = e^{j\theta}$. If the eigendecomposition corresponds to the true spectral matrix, then MUSIC spectrum $P_{MUSIC}(\theta)$ becomes equivalent to the polynomial on the unit circle and peaks in the MUSIC spectrum exist as roots of polynomial that lie close to the unit circle (Rao et al., 1989), (Cheng, 2005). That is:

$$P_{root-MUSIC}(z)|_{z=e^{j\theta}} = P_{MUSIC}(\theta) \tag{3.11}$$

Ideally, in the absence of noise, the poles will lie exactly on the unit circle at the locations determined by DOA. Ultimately, the polynomial is calculated and then the J roots that are inside the unit circle are selected. A pole of polynomial:

$$D(z)|_{z=z_q} = |z_q| = |e^{j \arg(z_q)}| \tag{3.12}$$

will result in a peak in the MUSIC spectrum at:

$$\theta = \sin^{-1}\{(\lambda/2\pi d)\arg(z_q)\} \tag{3.13}$$

3.4.4 Estimation of Signal Parameters via Rotational Invariance Technique (ESPRIT) Algorithm

ESPRIT was proposed by Roy and Kailath (Roy et al., 1986) and it is considered to be one of the most popular signal subspace based DOA estimation algorithm. This algorithm is more robust with respect to array imperfections than MUSIC (Khan et al., 2008). Computation complexity and storage requirements are lower than MUSIC as it does not involve extensive search throughout all possible steering vectors, but explores the rotational invariance property in the signal subspace created by two subarrays derived from original array with a translation invariance structure. It consists of three primary steps as follows (Chen et al., 2010):

- Signal subspace estimation
- Solution of the invariance equation and
- DOA estimation

After computing eigenvalues of the invariance equation, λ, the angle of arrival can be determined using:

$$\theta = \sin^{-1}\left(\frac{\arg(\lambda)}{2\pi d}\right) \tag{3.14}$$

3.4.5 Modified Forward Backward Linear Prediction (MFBLP) Algorithm

MFBLP is a high-resolution DOA estimation method proposed by Tufts and kumaresan (Tufts et al., 1982) which is suitable for short data lengths. The steps for carrying out this algorithm are summarized (Yuen et al., 1997) as follows:

- For each M x 1 steering vector $\hat{a}$estimated using some blind algorithm, form the matrix $2(M - L)$ x L matrix

$$Q = \begin{bmatrix} \hat{a}_{L-1} & \hat{a}_{L-2} & \dots & \hat{a}_0 \\ \hat{a}_L & \hat{a}_{L-1} & \cdots & \hat{a}_1 \\ \vdots & \vdots & \cdots & \vdots \\ \hat{a}_{M-2} & \hat{a}_{M-3} & \cdots & \hat{a}_{M-L-1} \\ \hat{a}_1^* & \hat{a}_2^* & & \hat{a}_L \\ \hat{a}_2^* & \hat{a}_3^* & & \hat{a}_{L+1} \\ \vdots & \vdots & & \vdots \\ \hat{a}_{M-L}^* & \hat{a}_{M-L+1} & & \hat{a}_{M-1} \end{bmatrix} \tag{3.15}$$

and the 2(*M*-*L*) x 1 vector

$$h = \begin{bmatrix} \hat{a}_L \\ \hat{a}_{L+1} \\ \vdots \\ \hat{a}_{M-1} \\ \hat{a}_0^* \\ \hat{a}_1^* \\ \vdots \\ \hat{a}_{M-L-1}^* \end{bmatrix} \tag{3.16}$$

Where $\hat{a}$ is the vector in the estimated steering vector $\hat{\boldsymbol{a}}$, M is the number of sensors and L must be chosen to satisfy the inequality:

$$G \leq L \leq M - \frac{G}{2} \tag{3.17}$$

- Take the singular value decomposition of Q as:

$$Q = U\Lambda V^H \tag{3.18}$$

- Then set $L - G$ smallest singular values on the diagonal of Λ to 0 and call it matrix Σ. The dimension of Σ is the same as that of Λ.

- Compute g as follows:

$$\boldsymbol{g} = [g_1 g_2 g_3 \ldots g_L]^{\mathrm{T}} = -\boldsymbol{V}\boldsymbol{\Sigma}^{\#}\boldsymbol{U}^{\boldsymbol{H}}\boldsymbol{h} \tag{3.19}$$

Then determine roots of the polynomial

$$H(z) = 1 + g_1 z^{-1} + g_2 z^{-2} + \ldots + g_L z^{-L} \tag{3.20}$$

Where the coefficients $\{g_1 g_2 g_3 \ldots g_L\}$ are the elements of the vector $\boldsymbol{g}$.

- The *G*zeros of $H(z)$ that lie on the unit circle, that is the zeros with magnitude 1, determines the unknown frequencies ω_k in (3.21), from which the DOA's angles can be computed.

$$\omega_k = \frac{2\pi f d \sin\theta_k}{c} \tag{3.21}$$

3.5 Fading Coefficient Estimation

After the realization of high-resolution techniques, the DOA angles (θ) in each group are calculated. Then, the fading coefficients belonging to each signal (actually belonging to each DOA angle) can be acquired by the procedure described in (Zhang et al., 2008), where the strongest coefficient in each group is normalized to unity. Mathematically, the fading coefficients for k^{th} frequency, $\boldsymbol{\rho_k}$, can be expressed as:

$$\boldsymbol{\rho}_{\mathbf{k}} = \begin{bmatrix} \rho_{(k-1)L+1} & \rho_{(k-1)L+2} & \cdots & \rho_{(kL)} \end{bmatrix}^T = \frac{\mathbf{A}_{\mathbf{k}}^{\dagger}\mathbf{a}_{\mathbf{k}}}{(\mathbf{u}\mathbf{A}_{\mathbf{k}}^{\dagger}\mathbf{a}_{\mathbf{k}})} \tag{3.22}$$

Where $\mathbf{u} = [1\ 0\ \ldots\ 0]_{1\times L}$, $\dagger$ is the Moore-Penrose inverse operator, $\mathbf{a_k}$ is the k^{th} column (steering vector) of the estimated array response matrix in JADE algorithm and $\mathbf{A_k}$ is defined as:

$$\mathbf{A}_{\mathbf{k}} = \begin{bmatrix} \mathbf{a}\left(\theta_{(k-1)L+1}\right) & \mathbf{a}\left(\theta_{(k-1)L+2}\right) & \cdots & \mathbf{a}\left(\theta_{kL}\right) \end{bmatrix} \tag{3.23}$$

3.6 Frequency Matching

In the final step, the frequency matching of the noncoherent groups are made. Actually, the frequencies $\{\omega_1, \omega_2, \ldots, \omega_K\}$ can be easily found by taking total signal on any antenna element and processing this signal with the high-resolution technique used in third step. However, the calculated frequencies may not be ordered properly with the estimation steering vectors in step 2 and DOA angles in step 3. For example, the frequency of ω_1 may correspond to the third group in terms of steering vectors and DOA angles. For this purpose, a procedure is developed to make a proper matching between estimated frequencies and signal group.

The signal data given in (3.1) can be rewritten in terms of frequencies for each antenna element as

$$\begin{aligned} \mathbf{x}_m &= \begin{bmatrix} x_m(0) & x_m(1) & \cdots & x_m(N_s) \end{bmatrix}^T \\ &= \begin{bmatrix} 1 & 1 & \cdots & 1 \\ e^{j\omega_1} & e^{j\omega_2} & \cdots & e^{j\omega_K} \\ \vdots & \vdots & \ddots & \vdots \\ e^{jN_s\omega_1} & e^{jN_s\omega_2} & \cdots & e^{jN_s\omega_K} \end{bmatrix} \begin{bmatrix} \alpha_{m1} \\ \alpha_{m2} \\ \vdots \\ \alpha_{mK} \end{bmatrix} \end{aligned} \tag{3.24}$$

Where α_{mk} is the superposition of fading coefficients times phase delay for the m^{th} antenna element and k^{th} frequency. As explained above, both frequencies $\{\omega_1, \omega_2,\ldots,\omega_K\}$ and α_{mk} can be calculated for each antenna element by using corresponding antenna element's data and high-resolution technique. The same α values can be estimated as $\hat{\alpha}_{mp}$ by using the estimated fading coefficients and DOA angles of p^{th} signal group such that:

$$\hat{\alpha}_{mp} = \sum_{n=(p-1)L+1}^{p\times L} \rho_n e^{j2\pi d(m-1)\sin\theta_n/\lambda} \tag{3.25}$$

Here, it is again important to indicate that due to disorder of steering vectors in JADE step, the first frequency with α_{m1} values may not be matched to first group with $\hat{\alpha}_{m1}$ values. Therefore, frequency-group matching is done with a simple comparison, which is described below:

$$\begin{aligned} &k^{th}\ frequency \Leftrightarrow p_{est}{}^{th}\ group\ \ if \\ &\min\left\|\boldsymbol{\alpha}_{\mathbf{k}} - \hat{\boldsymbol{\alpha}}_p\right\| \ is\ \ at\ \ p = p_{est}\ \ for\ \ p = 1,....,K \end{aligned} \tag{3.26}$$

Where

$$\begin{aligned} \boldsymbol{\alpha}_{\mathbf{k}} &= \left[\alpha_{1k} \quad \alpha_{2k} \quad \cdots \quad \alpha_{Mk}\right], \\ \hat{\boldsymbol{\alpha}}_p &= \left[\hat{\alpha}_{1p} \quad \hat{\alpha}_{2p} \quad \cdots \quad \hat{\alpha}_{Mp}\right] \end{aligned} \tag{3.27}$$

and $\|\ \|$ denotes the norm operator.

4. SIMULATIONRESULTS for DOA and FADING COEFFICIENTS WITH FREQUENCY MATCHING

This chapter is devoted to the analysis and comparison of different simulations for JA

DE base DOAs and Fading coefficients estimation algorithms as well as frequency matching to evaluate their performances. The estimation algorithms to be considered here include ESPRIT, root-MUSIC, MFBLP, Min-norm, and MUSIC. The root mean square is used as a metric to compare the performance of these algorithms.

4.1 Simulation of DOA Estimation algorithms

In all the simulations which are developed in MATLAB environment with, M = 12 antenna-element uniform linear array (ULA) with relative inter-element spacing of $d = \lambda / 2$ is considered, and N = 12 signals impinge on the array. K = 3 noncoherent groups each containing L = 4 coherent signals are considered. It is assumed that there are K = 3 different users in the wireless communication application having the carrier frequencies of 2420 MHz, 2425.5 MHz and 2432 MHz. In the receiver side, a mixer with local oscillator of 2400 MHz and a following suitable lowpass filter are used to down-convert these frequencies to 20 MHz, 25.5 MHz and 32 MHz. By taking the sampling frequency (rate) as 1 GHz (or 1 Gsamples/second), which can be easily realized with the current oscilloscopes or similar sampling devices, the normalized angular frequencies are calculated as ω_1 = 0.1256 rad, ω_2 = 0.1603 rad, ω_3 = 0.2012 rad for this simulation. The DOA angles and multipath fading coefficients for each group (coherent signals) are given in the table 4.1 below.

It can be observed from the table 4.1, that there are some angles being very close to each other. Again, it can also be observed that there is strong multi-path effect for each group that the fading coefficients have magnitudes close to each other. In the initial simulations, the number of snapshot is selected as N_s = 2000, and T = 50 independent trials are employed at signal-to-noise (SNR) level of 10 dB. Here, the signal is fixed and independent trials are achieved by just changing the additive noise to the signal.

Table 4.1: True values of DOAs and fading coefficients for the first, second and third groups

Group	*True DOAs (deg)*	*True Fading coeffs.*
First Group	**10**	**1**
	20	**-0.6426+0.7266j**
	28	**0.8677+0.0632j**
	45	**0.7319-0.1639j**
Second Group	**5**	**1**
	25	**-0.8262+0.4690j**
	35	**0.1897-0.8593j**
	55	**0.2049-0.7630j**
Third Group	**40**	**1**
	60	**-0.1681-0.9045j**
	15	**-0.7293-0.1750j**
	30	**0.6102+0.1565j**

The true arrival angles and mean values of estimated angles as the average of 50 trials for root-MUSIC, MFBLP and ESPRIT DOA methods are given in Table 4.2 while Fig. 4.1 and 4.2 give the spectrums for Min-norm and MUSIC respectively. The mean value of the DOAs is given as:

$$mean = \sqrt{\frac{1}{NT}\sum_{t=1}^{T}\left(\theta_n\left(k\right)\right)^2} \tag{4.1}$$

Table 4.2: True arrival angles and mean of estimated DOA angles for Ns=2000, M=12, T=50 trials and SNR=10dB case

True Angles (degrees)	**Mean of Estimated Angles with High Resolution Methods (degrees)**		
	Root-MUSIC	***MFBLP***	***ESPRIT***
10	**10.0843**	**10.0632**	**9.9997**
20	**20.5100**	**20.1556**	**20.1997**

True Angles (degrees)	Mean of Estimated Angles with High Resolution Methods (degrees)		
	Root-MUSIC	*MFBLP*	*ESPRIT*
28	27.5114	27.9078	27.8078
45	45.0938	45.0698	44.9773
5	4.9969	5.0030	5.0022
25	24.8704	24.8885	24.9980
35	34.8160	34.8742	35.0617
55	55.0399	55.0271	54.9718
40	39.8429	39.9967	39.9286
60	59.9566	59.9985	59.8564
15	15.0480	15.0256	14.9378
30	29.9608	30.0429	29.9803

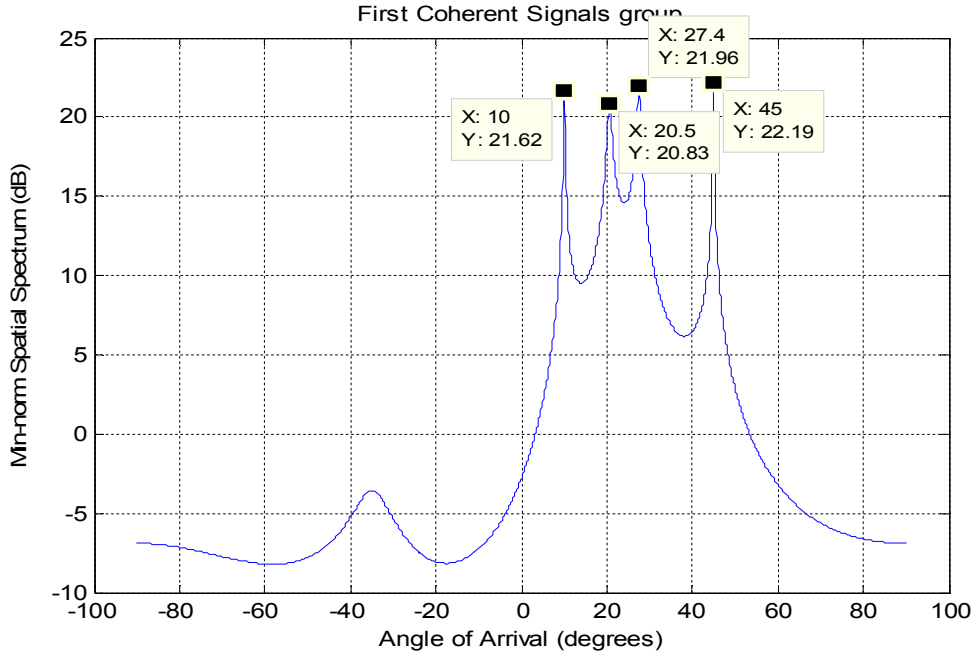

(a)

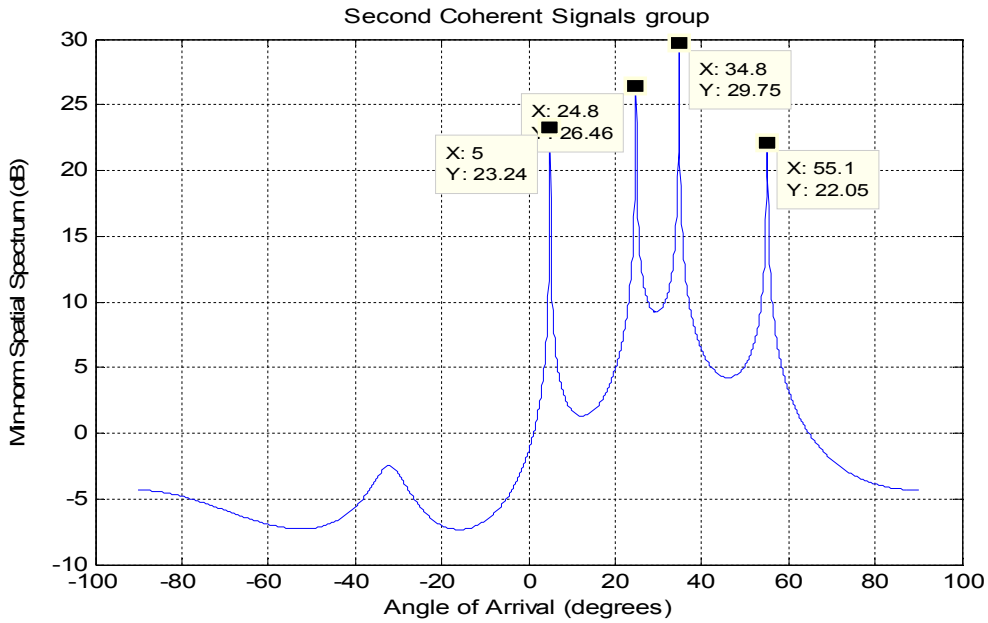

(b)

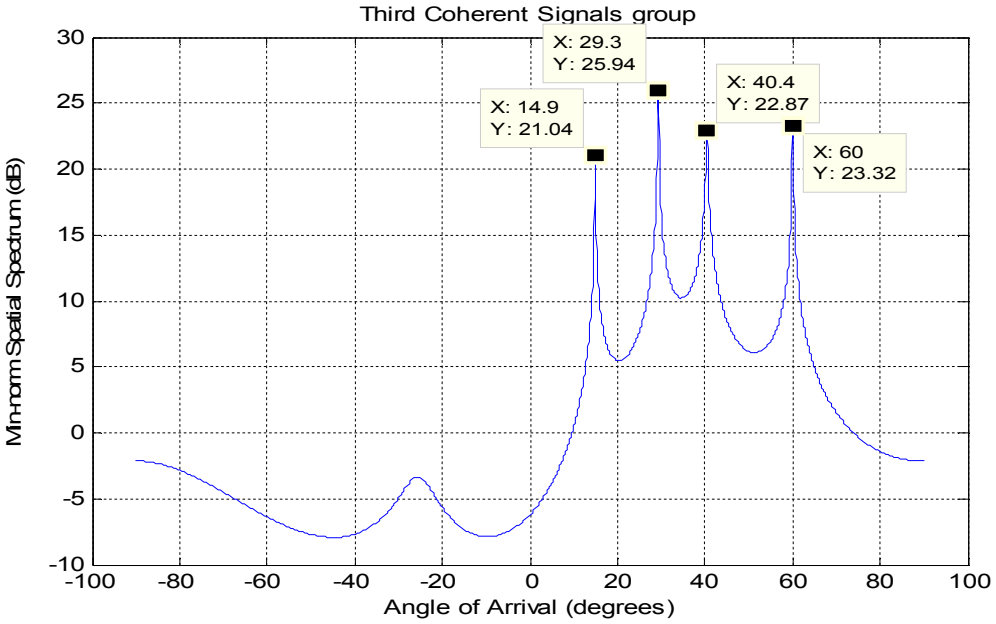

(c)

Figure4.1: The estimation of Min-norm spectrum for (a) the first signal group (b) the second signal group (c) the third signal group, for 50 Monte-Carlo trials. The high peaks indicate the estimated DOAs of the signals.

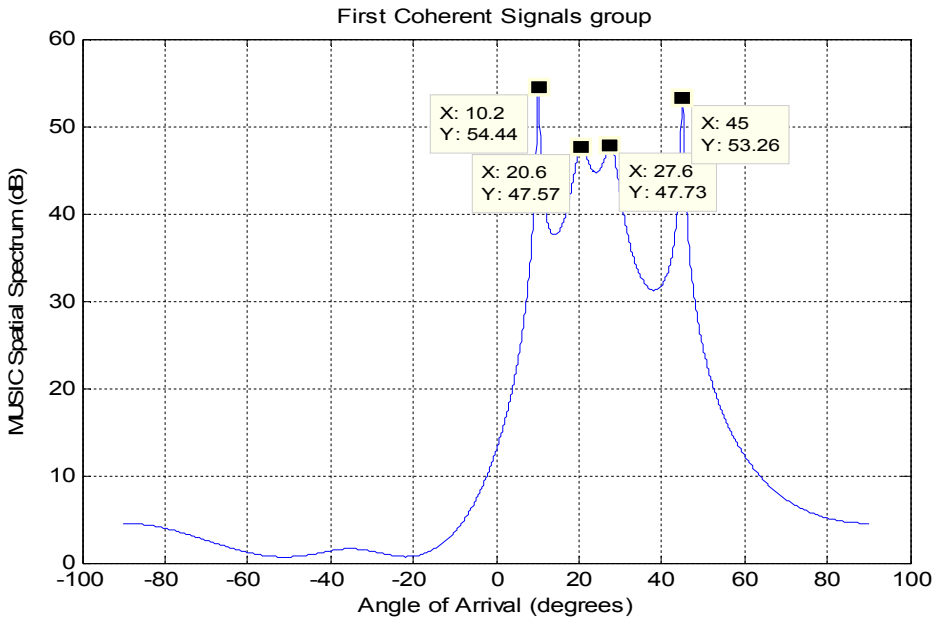
First Coherent Signals group
X: 10.2
Y: 54.44
X: 20.6
Y: 47.57
X: 27.6
Y: 47.73
X: 45
Y: 53.26
MUSIC Spatial Spectrum (dB)
Angle of Arrival (degrees)

(a)

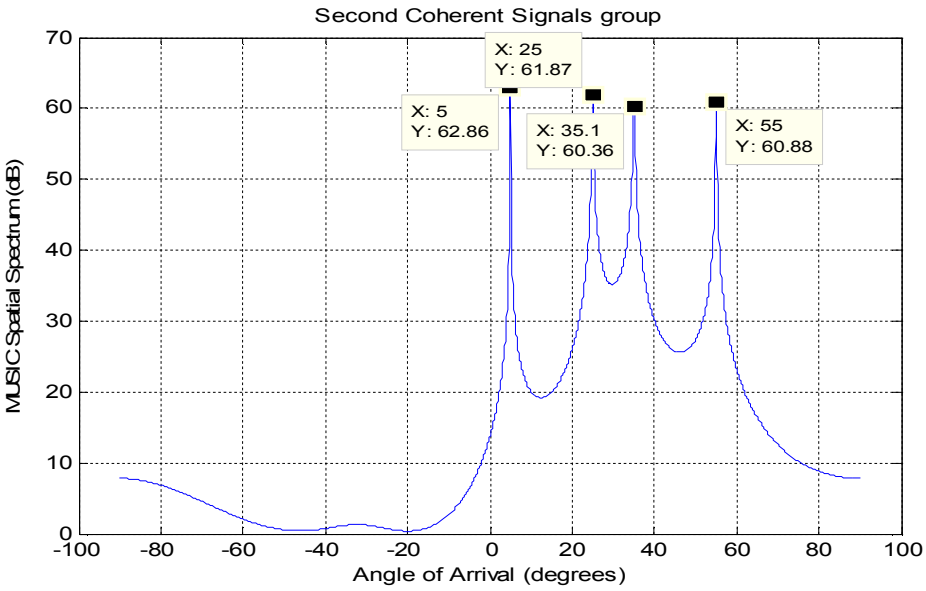
Second Coherent Signals group
X: 25
Y: 61.87
X: 5
Y: 62.86
X: 35.1
Y: 60.36
X: 55
Y: 60.88
MUSIC Spatial Spectrum (dB)
Angle of Arrival (degrees)

(b)

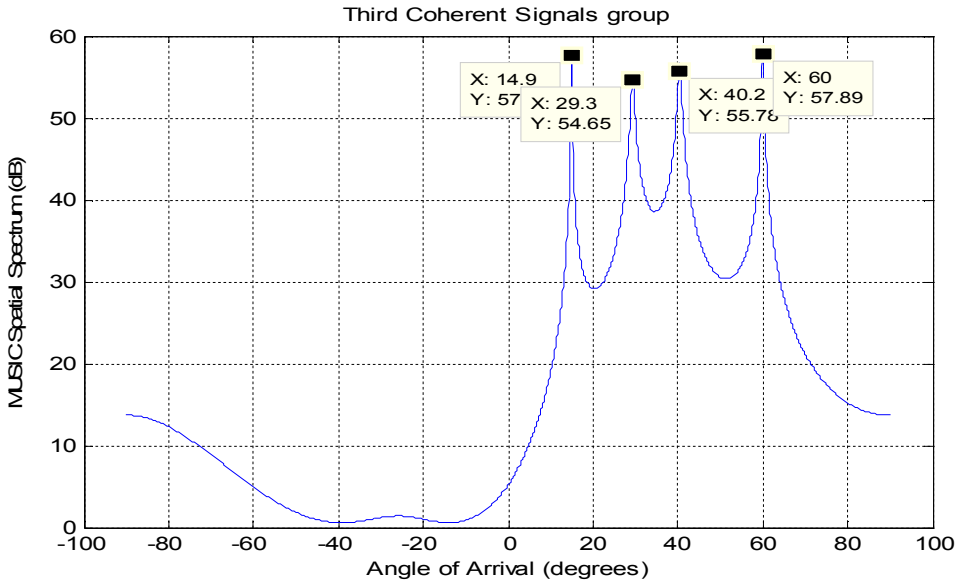

(c)

Figure4.2: The estimation of MUSIC spectrum for (a) the first signal group (b) the second signal group (c) the third signal group, for 50 Monte-Carlo trials. The high peaks indicate the estimated DOAs of the signals.

When the results in Table 4.1, Fig. 4.1 and 4.2 are analyzed, it can be deduced that both methods can be able to separate each non-coherent signal group correctly by the help of JADE algorithm, and have very good agreement with true angles even for moderate SNR level of 10 dB. While root-MUSIC algorithm has the inaccuracy (difference with the true angles) as high as 0.5 degrees, MFBLP and ESPRIT algorithms have the differences at most 0.15 and 0.2 degrees respectively, Min-norm and MUSIC each has maximum of 0.7 degrees.

4.2 Performance Comparison of DOAs and Fading Coefficients

For the accuracy performance, the JADE based DOA estimation methods are compared using the classical root mean square error (RMSE) for DOAs and fading coefficients given in (4.2) and (4.3) respectively. Figure 4.3, 4.4 and 4.5 show the variations of RMSE with SNR, number of array elements and number of snapshots respectively. The RMSE in DOA estimation is defined as (Yilmazer et al., 2006):

$$RMSE = \sqrt{\frac{1}{NT}\sum_{t=1}^{T}\sum_{n=1}^{N}\left(\hat{\theta}_n - \theta_n\right)^2} \qquad (4.2)$$

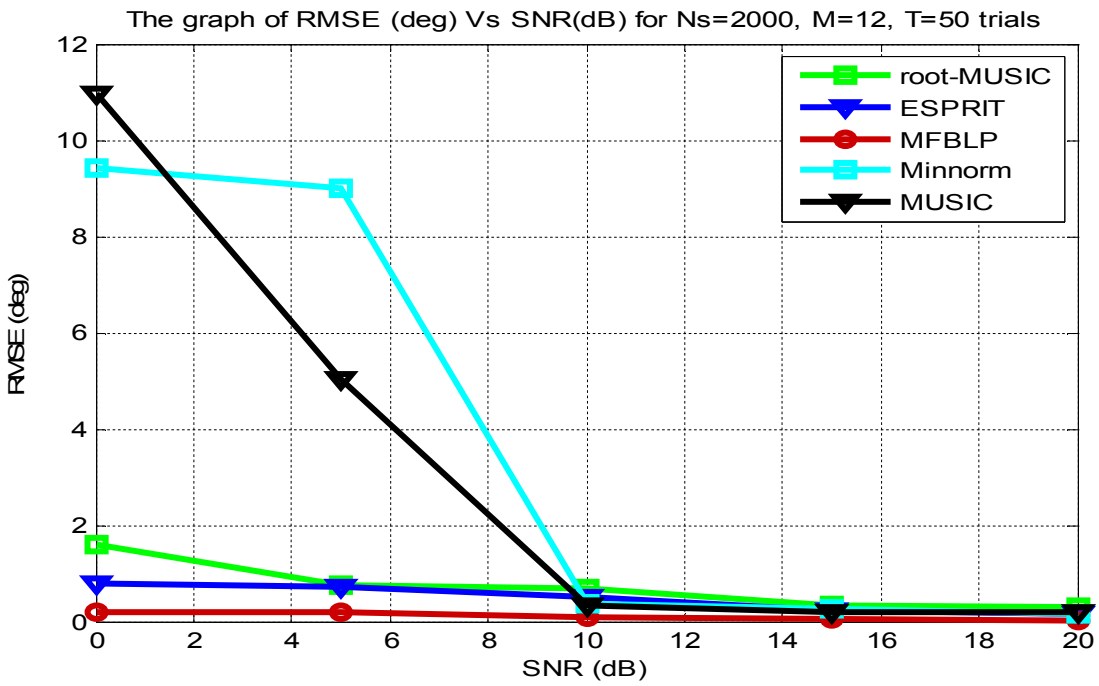

Figure 4.3RMSE for DOA estimation versus different SNR values for root-MUSIC, ESPRIT, MFBLP Min-norm and MUSIC algorithms.

According to simulation result in Fig. 4.3, RMSE values are found to be 0.1044, 0.5075, 0.6931, 0.3731 and 0.3302 for MFBLP, ESPRIT, root-MUSIC, Min-norm and MUSIC respectively at SNR=10dB. Therefore, it can be seen that although the mean (average) value performances of MFBLP, ESPRIT and root-MUSIC algorithms are close to each other, the variances belonging to Min-norm and MUSIC algorithm are significantly high as compared to MFBLP. So, the estimated values in Min-norm and MUSIC algorithms deviate (scatter) much more from the true values than MFBLP, ESPRIT and root-MUSIC.

The RMSE values of the DOA methods simulated for different number of antenna elements in the array are also evaluated for 50 trials at SNR level of 10 dB. The results are shown in Fig. 4.4. When the results in the figure is examined, both methods possess similar RMSE values and successful performances up to M being as low as 17. However, as the number of antenna array continues to reduce more, the RMSE results of the methods begin to differentiate clearly such that RMSE value at $M = 12$ for MFBLP is the lowest. Thus, the method with MFBLP again out performs the other methods at the low number of antenna elements in the array. It can be also concluded that MFBLP works well without the necessity of high number of antenna elements.

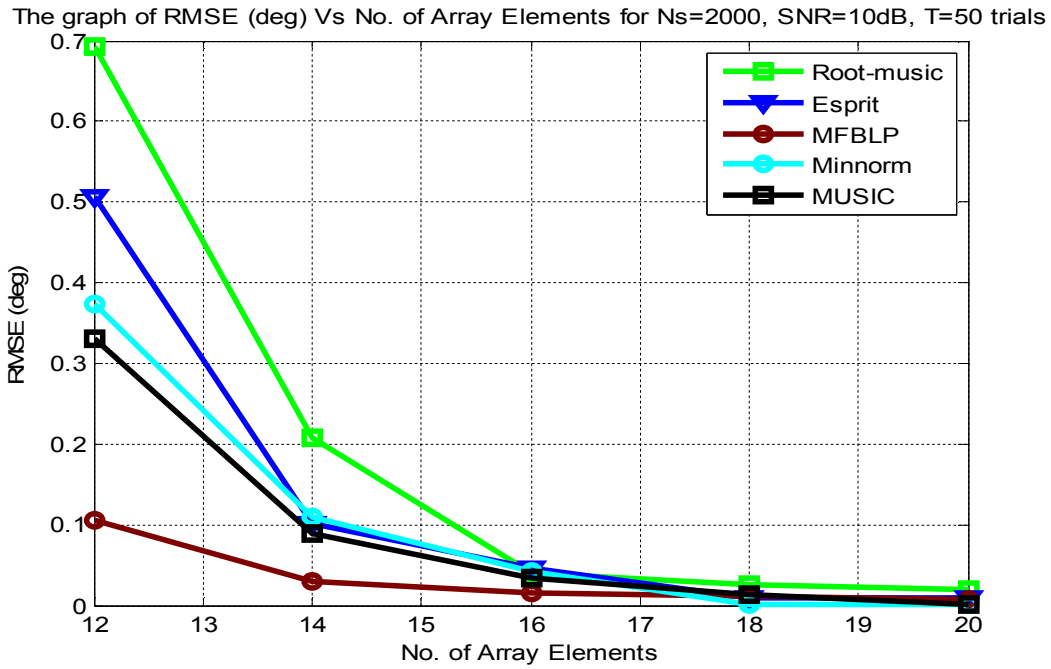

Figure 4.4RMSE for DOA estimation versus different Number of Array Elements values for root-MUSIC, ESPRIT, MFBLP Min-norm and MUSIC algorithms.

Another parametric analysis is carried out for the number of snapshots (samples) in the signal data. For this purpose, the additional simulations are done for N_s values of 500, 1000, 1500, 2000, 2500, and 3000 with fixed parameters of M = 12, SNR = 10 dB and T = 50 trials. The corresponding RMSE values are given in Fig. 4.5 for all DOA methods considered in this work. It is revealed from the results in the figure that the RMSE results of all the methods are almost constant and do not show a noticeable change as N_s decreases up to 1500. However, as N_s decreases 1000 and below, the effect of number of snapshots begins to be observed (in the way of increasing RMSE and consequently decreasing the performance). So, for this simulation example, the methods can be used at the minimum N_s of 1500 to get sufficient accuracy, and at N_s of 2000 to have the best performance. In addition, MFBLP has again better RMSE performance at all N_s values as compared to the other methods.

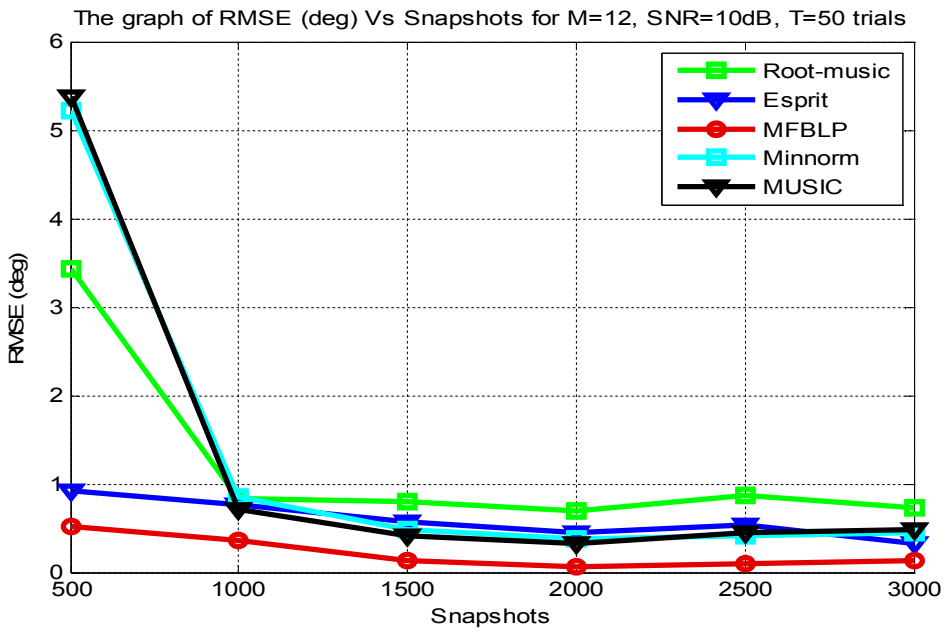

Figure 4.5RMSE for DOA estimation versus different Number of snapshots values for root-MUSIC, ESPRIT, MFBLP Min-norm and MUSIC algorithms.

As the final comparison of the DOAs and fading coefficients estimation methods, the root mean square error (RMSE) for fading coefficients estimation are compared for all the algorithms considered. Fig. 4. 6 through 5.8 show the variations of RMSE for fading coefficient with SNR, number of array elements and snapshots respectively. The RMSE in fading coefficient estimation is defined as (Yilmazer et al., 2006):

$$RMSE = \sqrt{\frac{1}{T\sum_{n=1}^{L}\|\rho_n\|^2}\sum_{t=1}^{T}\sum_{n=1}^{L}\|\hat{\rho}_n - \rho_n\|^2} \tag{4.3}$$

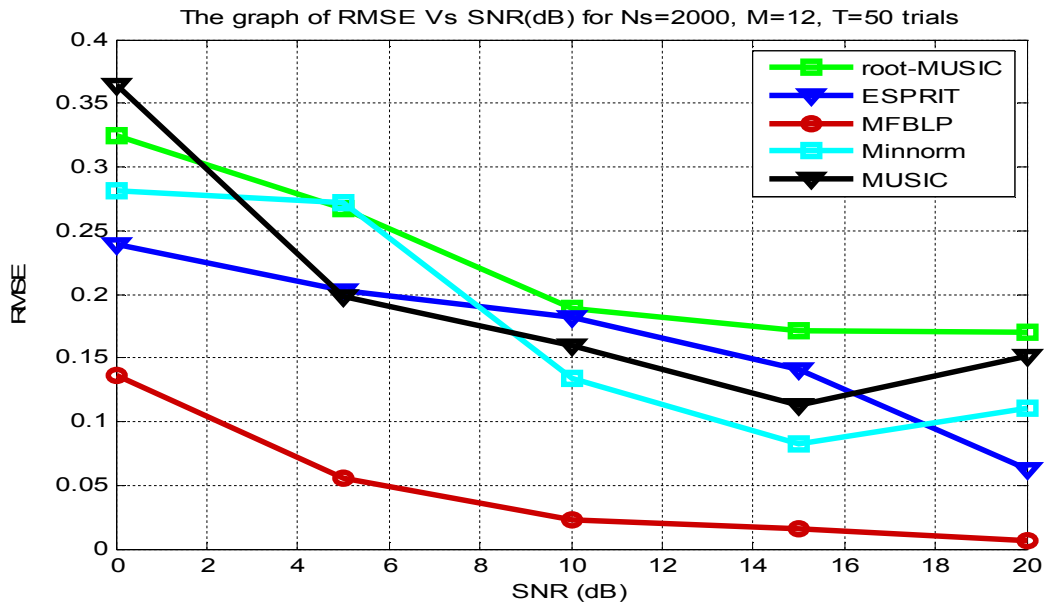

Figure 4.6RMSE for fading coefficients versus different SNR values for root-MUSIC, ESPRIT, MFBLP Min-norm and MUSIC algorithms.

It can seen from Fig. 4.6 above that all the methods considered deviated from the true fading coefficients values except MFBLP with lowest RMSE values for all the SNR values considered. MUSIC performance is the worst at lowest SNR of 0 dB.

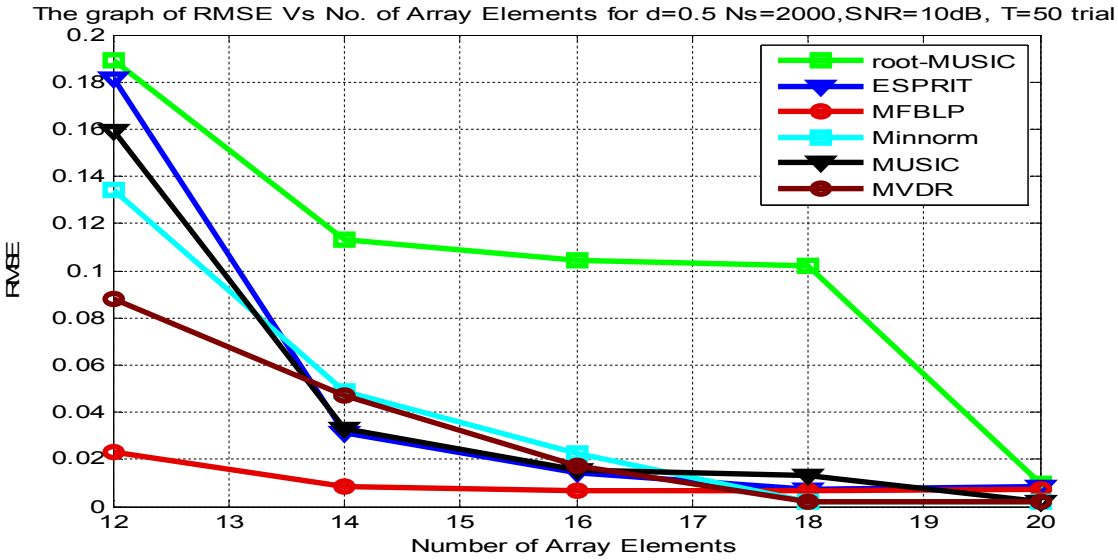

Figure 4.7RMSE for fading coefficients versus different Number of Array Elements values for root-MUSIC, ESPRIT, MFBLP Min-norm and MUSIC algorithms.

The high performance of MFBLP method is also observed here with less RMSE valuefor fading coefficients at 12 elements. Althogh all the methods show good performance towards estimating the fading coefficients, root-MUSIC performed worfully as the the number of array elements decreases from 20 to 12.

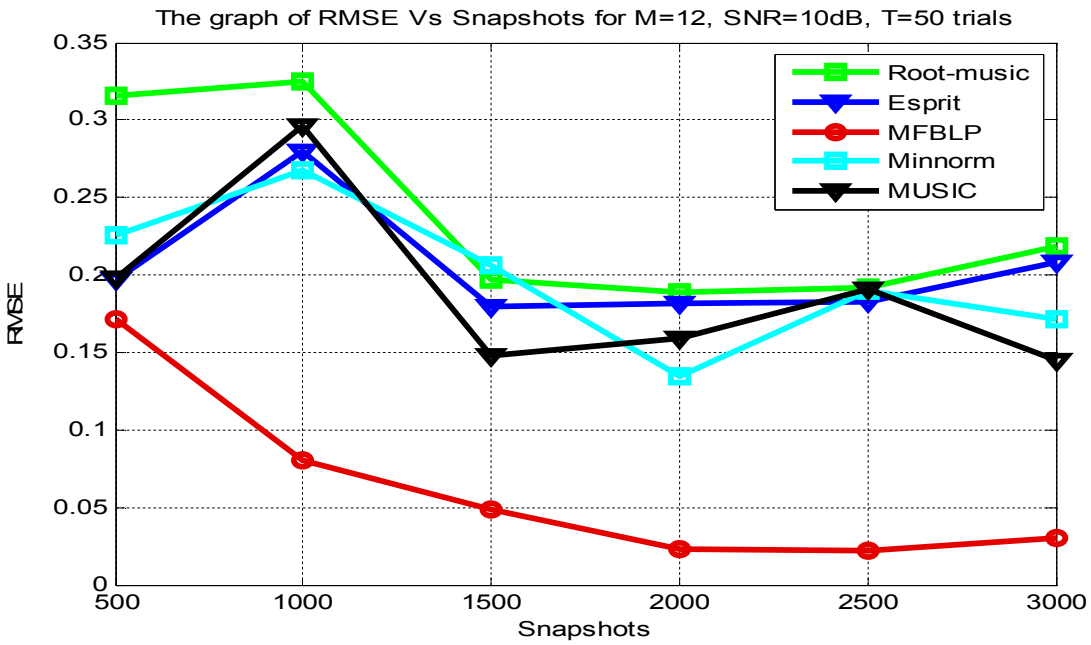

Figure 4.8RMSEfor fading coefficients versus different Number of snapshots values for root-MUSIC, ESPRIT, MFBLP Min-norm and MUSIC algorithms.

Lastly, the variation of RMS for fading coefficients with snapshots show a very good performace of MFBLP method as in Fig. 4.8. The other methods performances behaviour are roughly the same with worst at 1000 snapshots.

4.3 Comparison of Computation Time

In this part, computation time of JADE based root-MUSIC, ESPRIT, MFBLP, Min-norm, and MUSIC algorithms are compared for a single iteration and the results are shown in Table 4.3. These results were obtained in MATLAB environment with a HP Personal Computer, which has Intel Core i3-2328M processor at 2.2GHz and 4GB (929 usable) Ram.

Table 4.3: Comparison of Computation Time of JADE based root-MUSIC, ESPRIT, MFBLP, Min-norm, and MUSIC algorithms

	Root MUSIC	**ESPRIT**	**MFBLP**	**Min-nor**	**MUSIC**
Run Time/Iteration (second)	**5.088345**	**5.069575**	**4.983721**	**5.585365**	**5.600133**

The results show that MFBLP has the lowest run time followed by ESPRIT algorithm while Min-norm took the longest time to produce the required result.

4.4 Analysis of Frequency Matching Result

The simulation results of frequencies and groups matching are discussed here. For this purpose, the steps described in from (3.24) to (3.27) are followed, and the corresponding accuracy rates of correct matching are obtained. For instance, for the case of N_s = 2000, M = 12, SNR = 10 dB and DOA method of ESRPIT, the norms of differences (as described in (3.26)) between the fading coefficient vector for the normalized angular frequency of ω_3 = 0.2012 rad/s or the frequency of 32 MHz (k =3) and the fading coefficient vectors for first, second and third groups (p = 1, 2 and 3) are calculated as 0.02966, 8.0079 and 9.1710, respectively. Correspondingly, ω_3 (or f_3) is assigned as the frequency of first signal group. Then, the DOA angles in the assigned source group are compared with the true angles of the matched frequency. If the difference in root-mean-square sense is smaller than 5 degrees (i.e. it is lower than 1 degree for the above example), the matching is classified as "correct"; otherwise, it is "incorrect" if it is higher than 5 degrees. By this outlined approach, the simulations are performed at several SNR levels with 50 trials and the given DOA algorithms. The accuracy rates of the "correct" matching are depicted in Table 4.4 and Fig. 4.9.

Table4.4: variation of Number of correct frequency matching (%) with SNR

SNR(dB)	Root-MUSIC	ESPRIT	MFBLP	Min-norm	MUSIC
	NO. of correct freq. Matching (%)	NO. of correct freq. Matching (%)	NO. of correct freq. Matching (%)	NO. of correct freq. Matching (%)	NO. of correct freq. Matching (%)
0	86.6667	100	100	66.6667	46.6667
5	80	100	100	80	73.3333
10	100	100	100	93.3333	80
15	100	100	100	93.3333	86.6667
20	100	100	100	93.3333	93.3333

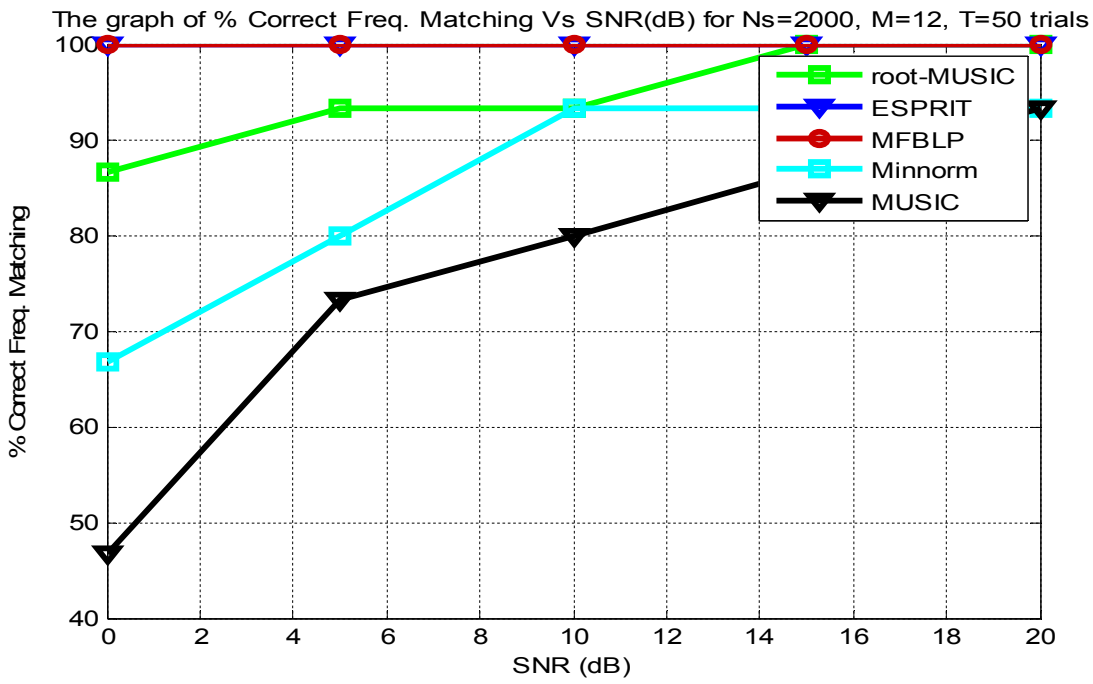

Figure 4.9 Percentages of "correct" matching versus different SNR levels for root-MUSIC, ESPRIT and MFBLP algorithms.

While MFBLP and ESPRIT algorithms have 100 percent accurate matching rates even at the low SNR level of 0 dB, root-MUSIC achieves 100 percent up to SNR = 15 dB, and can still give accuracy rate higher than 86 percent at SNR = 0 dB. Min-norm and MUSIC have the same percentage of 93 percent at 20 dB with MUSIC having the least accuracy rate of slightly above 46 percent at 0dB .

5. BEAMFORMING

Beamforming is the method used to create the radiation pattern of the antenna array by adding constructively the phases of the signals in the direction of the targets/mobiles desired, and nulling the pattern of the targets/mobiles that are undesired/interfering targets.

By using beamforming algorithms, the weight of antenna arrays can be adjusted to form certain amount of adaptive beam to track corresponding users automatically and at the same time to minimize interference arising from other users by introducing nulls in their directions (Nwalozie et al., 2013).

5.1 Beamforming Algorithms

Adaptive beamforming algorithms are classified base on the assumptions on the desired signals. The first classification considers that part of the signal is known through training sequence. This known signal is then compared with what is received, and the weights are then adjusted to minimize the Mean Square Error (MSE) between the known and the received signals (Poluri et al., 2013). This class of beamforming algorithms mitigate multipath fading as well as interference since the weights are updated according to the incoming signals. The second class uses the knowledge of the incoming signal to identify all angles of arrivals and then adjust the complex weights to produce a main lobe towards the signal of interest (SOI) and nulls toward signal not of interest (SNOI).

In this thesis, twobeamforming algorithms are considered. They include, least mean square (LMS) and normalized least mean square (NLMS).

5.1.1 Steepest Descent

The steepest descent method of searching the performance surface has been widely used due to its ease of implementation. In this method, all components of the complex weight vector are changed in accordance with the direction of the negative gradient of the surface at each iteration. Moving in the direction of the negative gradient leads toward the minimum as long as the origin lies on one of the principal axis of the surface.

The steps of steepest descent algorithm can be summarized as follows (Poularikas et al., 2006).

Step-I: Algorithm starts with the initial value assignment *w(0)*, which is usually equal to null vector.

Step-II: Gradient vector $\nabla_n(w(0))$ is computed.

Step-III: To obtain *w(1)*, $-\mu\nabla_n(w(0))$ is calculated and added to *w(0)*.

Step-IV: After that go to Step-II and continue the process to find optimum coefficients (until $\nabla_n(w(0))$ is equal to zero)

The method of steepest descent can be expressed in the form of the following iterative equation:

$$w(n+1) = w(n) + \mu(-\nabla_n) \tag{5.1}$$

whereμ is a constant that regulates the step-size, and ∇_n is the gradient of the surface.

5.1.2 Least Mean Square Algorithm

The LMS algorithm is the most widely used adaptive beamforming algorithm so far because of its low computational complexity and robustness, though its main draw back is its requirement for many iterations before satisfactory convergence is achieved. The algorithm was derived by Widrow and Hoff (Haykin, 1991) in1959. The Least Mean Square (LMS) algorithm uses a gradient based method of steepest decent (Kawitar et al., 2005) and it is based on the knowledge of the incoming signal. It involves new observations and iteratively minimizes linearly the mean square error between the estimated and desired signals. The LMS algorithm equation for updating the weights of the beamformer is expressed as(Haykin, 1991):

$$w(n+1) = w(n) + \mu e(n) x^*(n) \tag{5.2}$$

Where x(n) and w(n) are the input signal and weight respectively and also μ is the step-size parameter which controls the immediate change of the updating factor.

The step-size parameter has significant effect on the LMS algorithm for that, if it is very small, the convergence to optimal solution takes longer time

while if it is high, the stability of the system is lost. For stability, the following condition (Haykin, 1991) must be satisfied:

$$0 < \mu < \frac{1}{\lambda_{max}} \tag{5.3}$$

Where λ_{max} is the maximum eigenvalue of the autocorrelation matrix.

The error signal is also express as (Schmidt et al., 1986):

$$e = d - w^H x \tag{5.4}$$

Where *d* and *w* are the desired signal and complex weight respectively

5.1.3 Normalized Least Mean Square Algorithm

Normalized Least Mean Square (NLMS) is actually derived from Least Mean Square (LMS) algorithm. The need to derive this NLMS algorithm is that the input signal power changes in time and due to this change the step-size between two adjacent coefficients of the filter will also change and also affect the convergence rate. Due to small signal's power this convergence rate will slow down and due to high signal's power this convergence rate will increase and give an error. So to overcome this problem, the step-size parameter is adjusted with respect to the input signal power. Therefore the step-size parameter is said to be normalized. The step-size for NLMS adaptive beamforming algorithm is given by (5.5) below (Haykin, 1991):

$$\mu(n) = \frac{\beta}{c + \|x(n)\|^2} \tag{5.5}$$

Where β is the normalized step-size with boundary given in (5.6) and c is a small positive number that keeps the step-size as minimum as possible when x(n) is very small.

$$0 < \beta < 2 \tag{5.6}$$

Therefore, the weight updating equation for NLMS algorithm can be expressed as;

$$w(n+1) = w(n) + \frac{\beta}{c + \|x(n)\|^2} e(n) x^*(n) \tag{5.7}$$

The problem of gradient noise amplification is avoided in NLMS. For instant, when **x**(n) is too large, the error becomes significant in LMS and the performance degraded, but using NLMS, the error becomes minimal as the input signal power increases due to norm term plus the constant c in the denominator of the complex weight updating equation.

5.2 The Measure for Performance Evaluation of Beamforming Algorithms

After the optimum excitation coefficients of each antenna elements are obtained by steepest descent, LMS and NLMS algorithms, the normalized array factor (AF_n) of the antenna array is calculated. Next, the degradation in desired signal power level is evaluated with a new measure of "power down in dB". In this measure, the power difference in dB between maximum available power and power with optimized coefficients in the worst case is used. The received power in dB for each group can be given as:

$$P(dB) = 20\log_{10}\left|\rho_d AF_n(\theta_d) + \sum_{i=1}^{L-1} \rho_{i,u} AF_n(\theta_{i,u})\right| \tag{5.8}$$

where ρ_d and $AF_n(\theta_d)$ are fading coefficient and normalized array factor at DOA of desired signal, respectively; and $\rho_{i,u}$ (where $|\rho_{i,u}| < 1$) and $AF_n(\theta_{i,u})$ for i=1,…, L-1 are those of undesired signals. In mobile wireless communication systems, although the magnitudes of fading coefficients change slowly, the phase terms are very sensitive especially to the relative distances between sources and antennas such that the phase value can jump 180 degrees even with a small change in the distance. Therefore, the phase terms of undesired signals' contributions in the summation in (5.8) can all be out of phase relative to desired signal, which results in reduction at the power level of desired signals. By assuming $\rho_d = 1$ and $AF_n(\theta_d)=1$, this worst power (P_w) can be expressed as:

$$P_w(dB)=\begin{cases}20\log_{10}\left(1-\sum_{i=1}^{L-1}\left|\rho_{i,u}\right|\left|AF_n\left(\theta_{i,u}\right)\right|\right), & if \sum_{i=1}^{L-1}\left|\rho_{i,u}\right|\left|AF_n\left(\theta_{i,u}\right)\right|\le 1\\ -\infty\, dB & ,if \sum_{i=1}^{L-1}\left|\rho_{i,u}\right|\left|AF_n\left(\theta_{i,u}\right)\right|>1\end{cases} \quad (5.9)$$

Regardingly, for nonzero fading coefficients of undesired signals, the theoretical maximum available power can be only achieved when a maximum in AF is at the DOA of desired signals ($AF_n(\theta_d)=1$), and minima (nulls) are at the DOA of undesired signals ($AF_n(\theta_{i,u})=0$). So, according to (5.8), P_{max}(dB) becomes 0 dB, and the power down in dB can be formulated as:

$$P_{down}(dB)=P_{\max}(dB)-P_w(dB)=0-P_w(dB) \quad (5.10)$$

Here, for instance, 3 dB of P_{down} means the loss of half of the power of the desired signal, and ∞ dB of P_{down} corresponds to no received desired signal.

As an example, the simulation carried out here has the fading coefficients as shown in table 5.1, which were obtained from DOA and fading coefficients estimation using MFBLP algorithm in chapter 4.

Table 5.1: estimated fading coefficients

First Group	Second Group	Third Group
0.7315 - 0.1603*i	0.2036 - 0.7633*i	-0.7266 - 0.1796*i
1.0000	1.0000	0.1625 – 0.9024*i
0.8635 + 0.0708*i	-0.8157 + 0.4752*i	1.0000
0.6480 + 0.7153*i	0.1818 - 0.8695*i	0.6072 + 0.1588*i

Here, the fading coefficient of 1 at each group belongs to desired signal and other coefficients are for undesired ones. Since the sum of magnitudes of the fading coefficients of undesired ones is greater than 1 for each group, by considering (5.9) it has a possibility of receiving no desired signal (power down of ∞ dB) with the random changes of phases when no adaptive beamforming is employed.

6. SIMULATIONS and RESULTS for BEAMFORMING

In this chapter, the simulations for different adaptive beamforming algorithms are carried out

6.1 Adaptive Beamforming Simulation Results

After successful estimation of DOAs and fading coefficients with different DOA estimation algorithms discussed in chapter 3 and 4, the values of the DOAs and fading coefficients obtained from the best algorithm, MFBLP, as shown in the table 6.1 are used to adaptively optimize the excitation coefficients of the antenna array with M = 12, N_p = 500 and step-size, μ = 0.0014 for LMS and steepest descent and β=0.42 for NLMS.

Table 6.1: Estimated values of DOAs and fading coefficients for the first, second and third signal groups obtained using MFBLP algorithm

Group	***Estimated DOAs (deg)***	***Estimated Fading coeffs.***
First Group	**10.0632**	**0.7315 - 0.1603*j**
	20.1556	**1.0000**
	27.9078	**0.8635 + 0.0708*j**
	45.0698	**0.6480 + 0.7153*j**
Second Group	**5.0030**	**0.2036 - 0.7633*j**
	24.8885	**1.0000**
	34.8742	**-0.8157 + 0.4752*j**
	55.0271	**0.1818 - 0.8695*j**
Third Group	**39.9967**	**-0.7266 - 0.1796*j**
	59.9985	**-0.1625 - 0.9024*j**
	15.0256	**1.0000**

The MATLAB simulation results of adaptive beamforming algorithms, steepest descent, least mean square (LMS) and normalized least mean square (NLMS) discussed in chapter 5 are given in this section and also comparative analysis of each algorithm with regard to power reduction in the signal power level is carried out. The MATLAB codes in Balanis' Book (Balanis, 2005) are benefitted from and modified for the testing purpose of this research work.

6.1.1 Steepest Descent Algorithm Simulation Result

The Fig. 6.1 and 6.2 below show the polar and rectangular radiation pattern respectively, of the first, second and the third group using steepest descent method for adaptive beamforming.

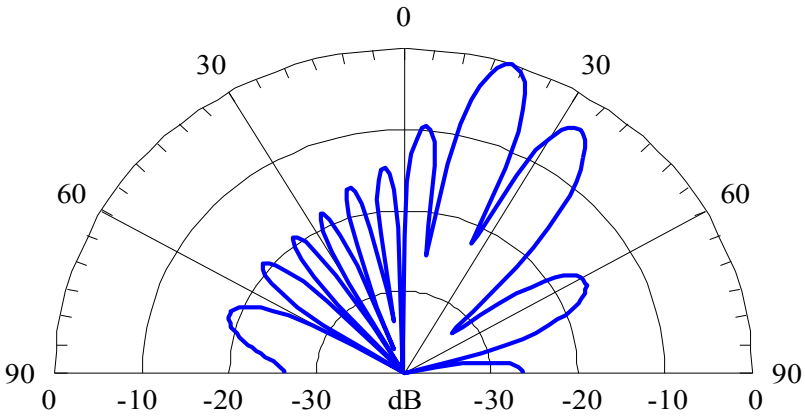

(a)

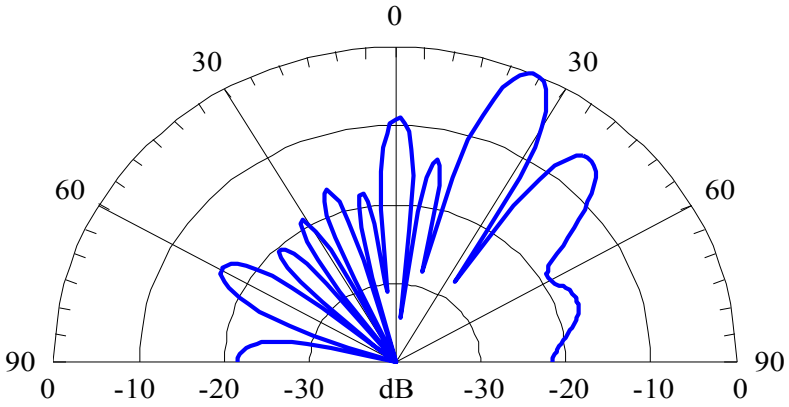

(b)

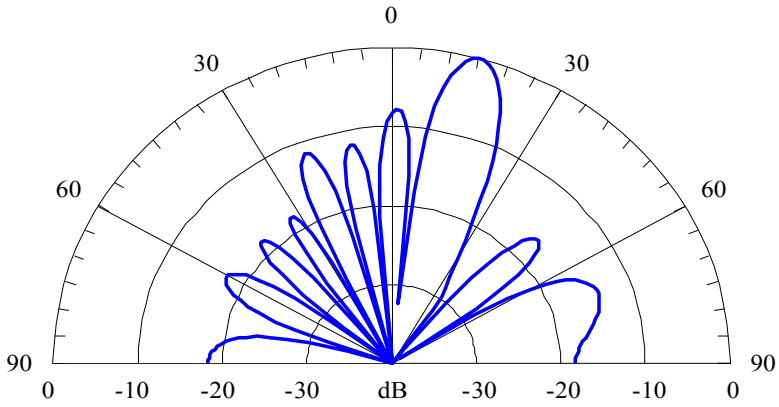

(c)

Figure 6.1 Radiation pattern of the adaptive beamforming using Steepest Descent algorithm for (a) the first signal group (b) the second signal group (c) the third signal group

It is clear from the radiation patterns in Fig. 6.1and 6.2 that, steepest descent method produces a lot of sidelobes that have powers just below the main lobe and this could be regarded as the source of interference to the main lobe.

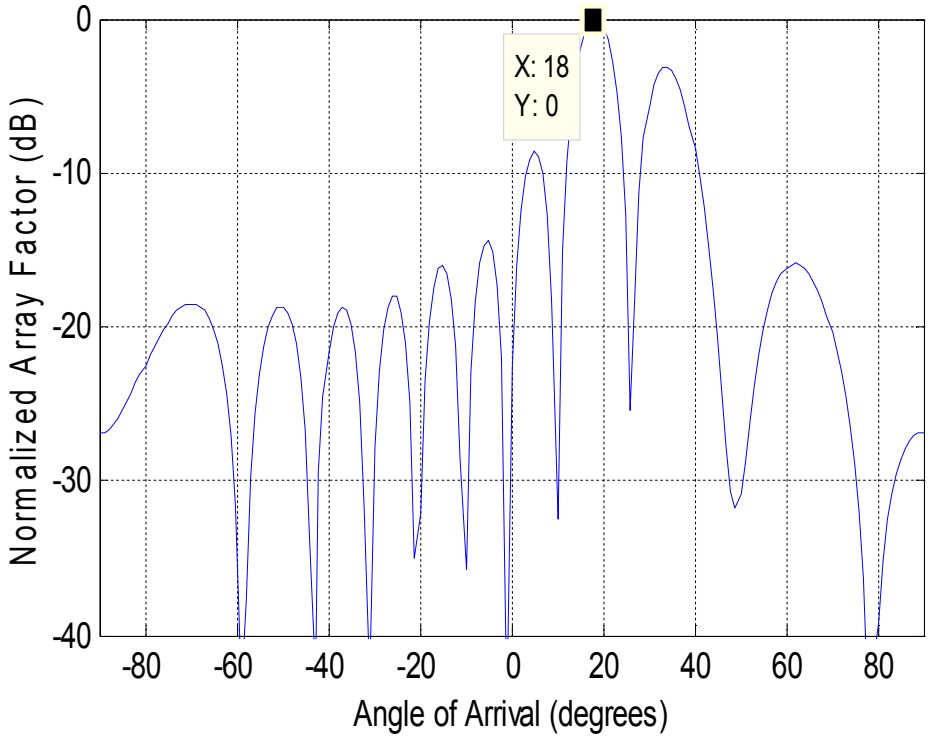

(a)

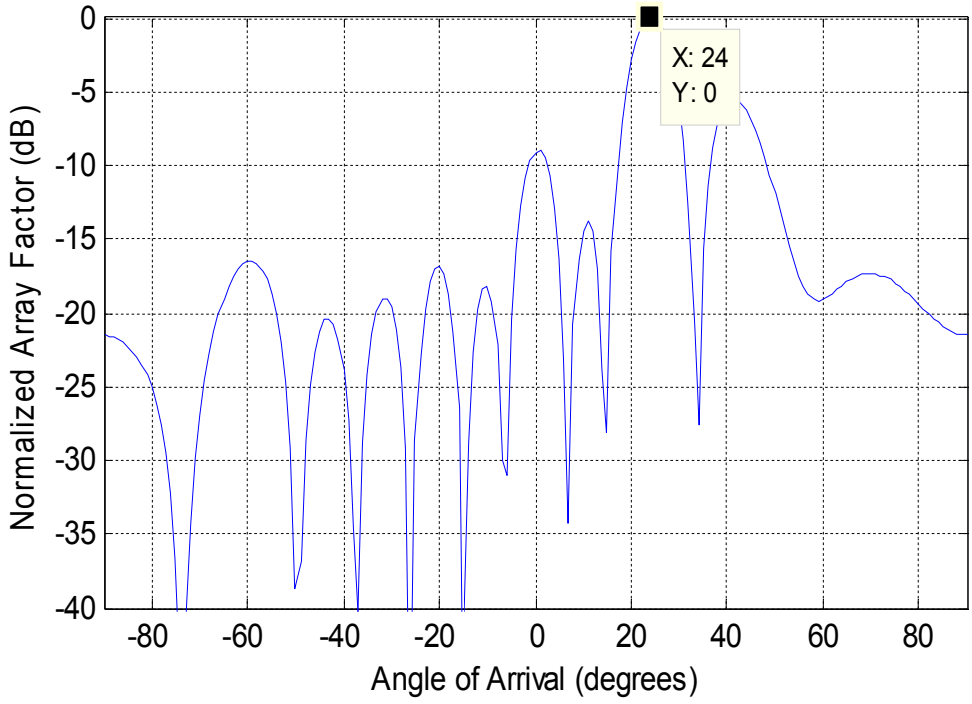

(b)

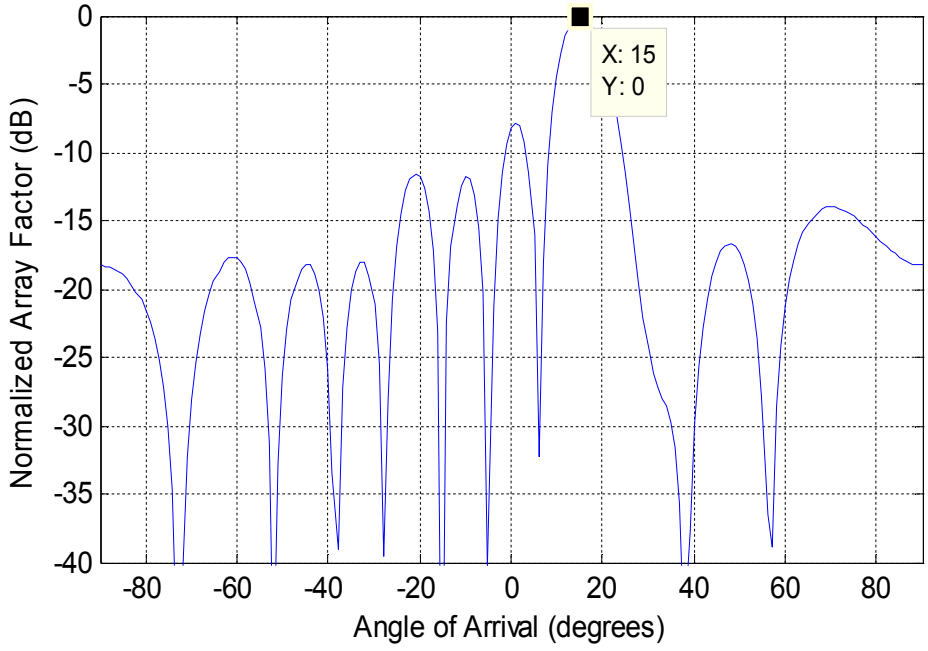

(c)

Figure 6.2, Array factor verses Angle of Arrival for (a) the first signal group (b) the second signal group (c) the third signal group using Steepest Descent algorithm

As shown in Fig. 6.2 above, the method has identified the SOI as 18^0, 24^0 and 15^0 for the first, second and third signal groups respectively.

6.1.2 Least Mean Square Algorithm Simulation Result

The normalized polar plot of the radiation patterns for the first, second and third signal groups with least mean square (LMS) algorithm are given in Fig. 6.3

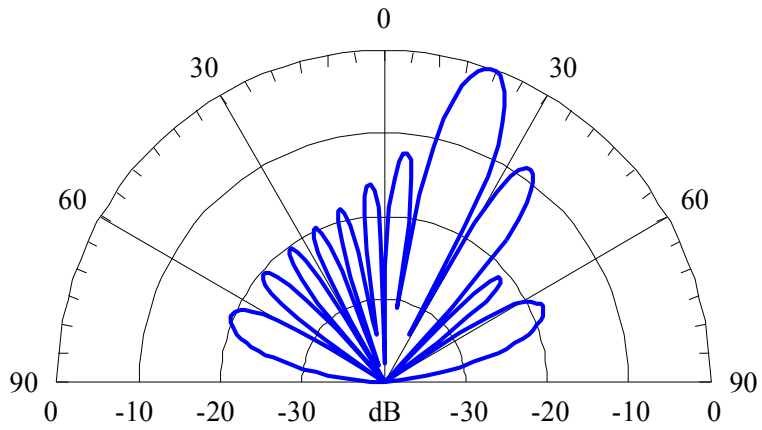

(a)

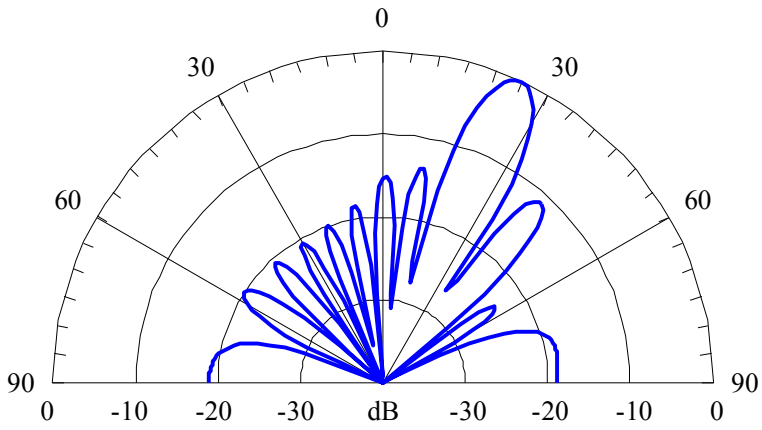

(b)

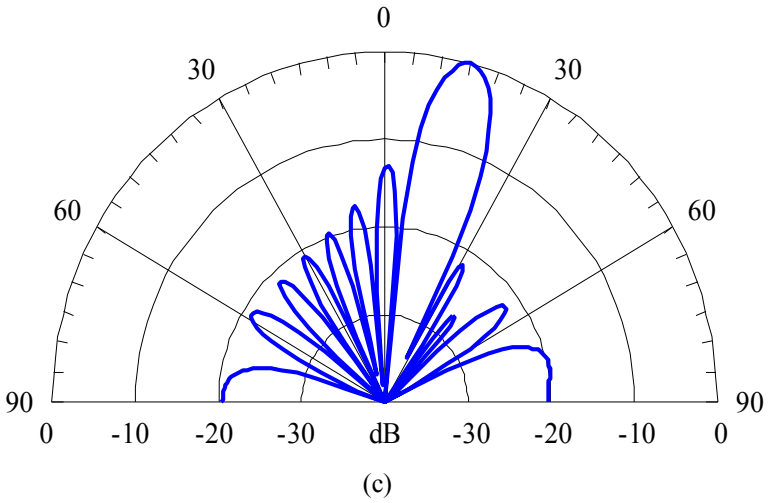

Figure 6.3 Radiation pattern of the adaptive beamforming using LMS algorithm for (a) the first signal group (b) the second signal group (c) the third signal group

In Fig. 6.3, it can clearly be seen that the main lobes of the adaptive beamforming patterns are directed toward the angles of signal of interest (SOI) in all the three groups, which are 20^0, 25^0 and 15^0in the first, second and third groups, respectively; while all other angles of the signals or signal not of interest (SNOI) are directed toward the nulls.

The array factor verses angle of arrival for the first, second and third signal groups are also shown in Fig. 6.4.

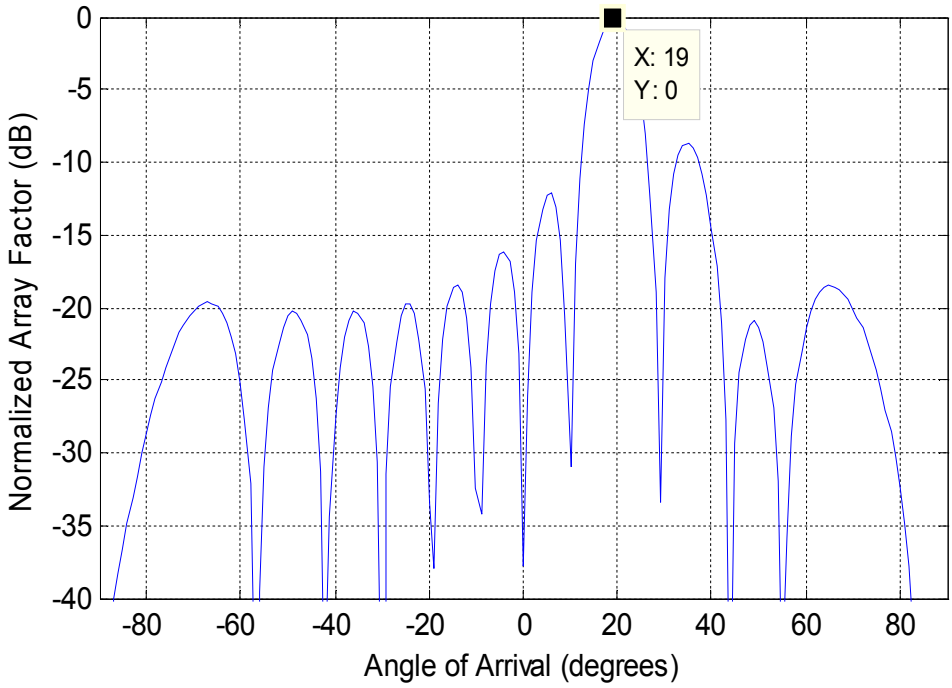
X: 19
Y: 0
Normalized Array Factor (dB)
Angle of Arrival (degrees)
0
-5
-10
-15
-20
-25
-30
-35
-40
-80
-60
-40
-20
0
20
40
60
80

(a)

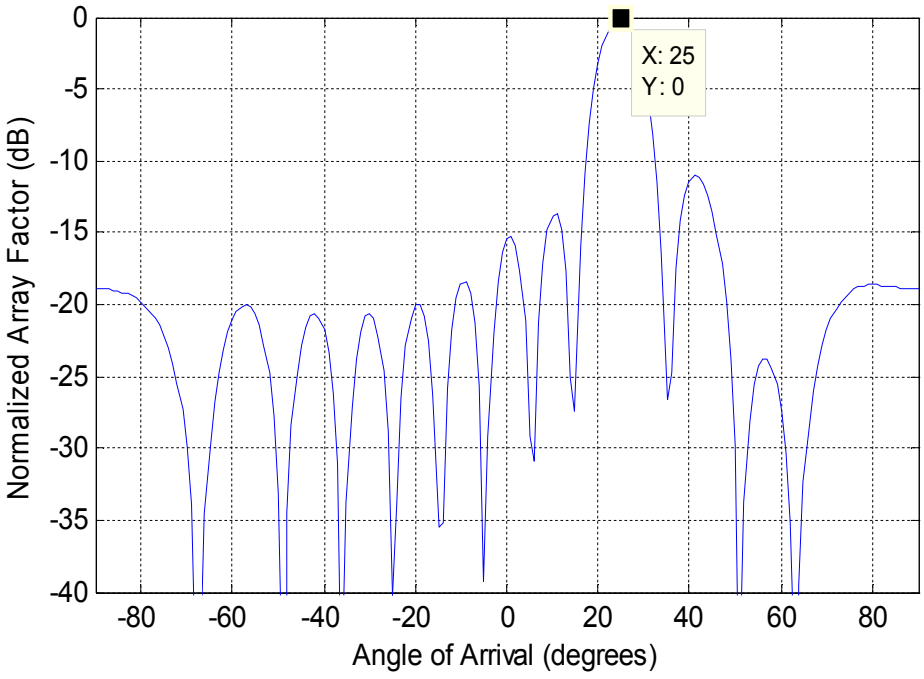
X: 25
Y: 0
Normalized Array Factor (dB)
Angle of Arrival (degrees)
0
-5
-10
-15
-20
-25
-30
-35
-40
-80
-60
-40
-20
0
20
40
60
80

(b)

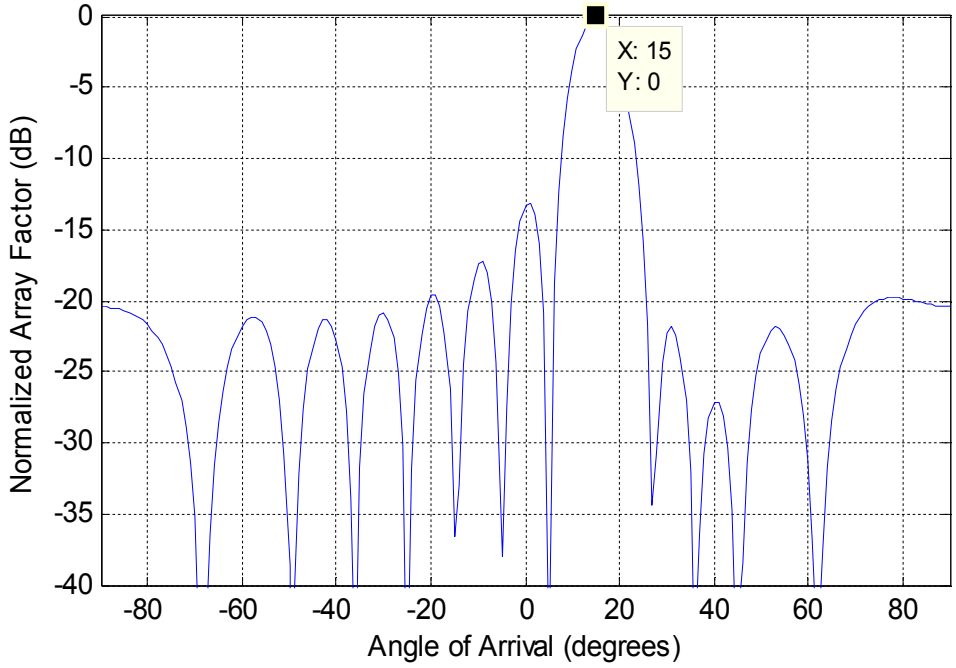

(c)

Figure 6.4, Array factor verses Angle of Arrival for (a) the first signal group (b) the second signal group (c) the third signal group using LMS algorithm

6.1.3 Normalized Least Mean Square Algorithm Simulation Result

The normalized polar plot of the radiation patterns and array factor verses angle of arrival for the first, second and third signal groups with normalized least mean square error (NLMS) algorithm are given in Fig. 6.5 and 6.6 respectively.

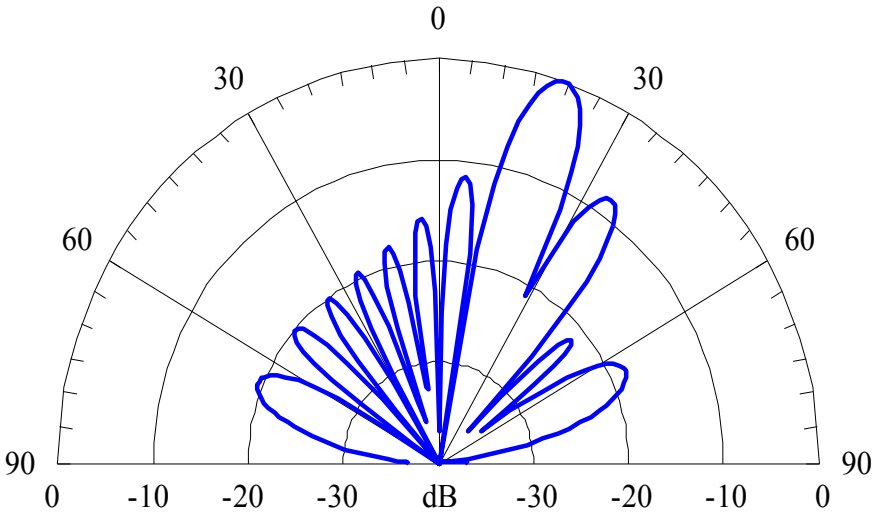

(a)

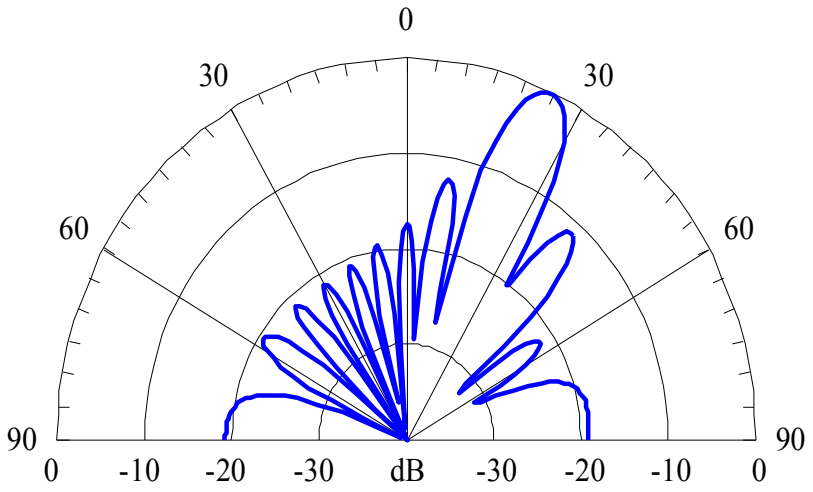

(b)

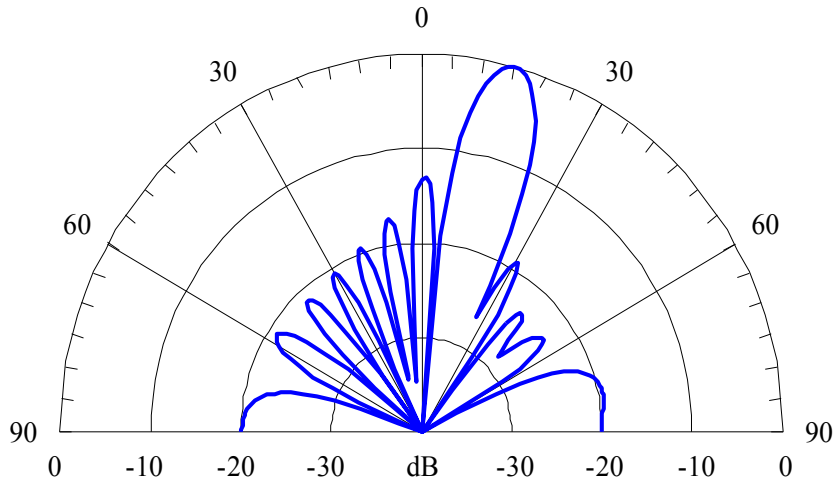

(c)

Figure 6.5, Radiation pattern of the adaptive beamforming for (a) the first signal group (b) the second signal group (c) the third signal group using NLMS algorithm

Here also the aim of beamforming is achieved by directing the main lobes of the adaptive beamforming patterns toward the angles of signal of interest (SOI) in all the three groups, which are 20^0, 25^0 and 15^0in the first, second and third groups, respectively; while all other angles of the signals or signal not of interest (SNOI) are directed toward the nulls.

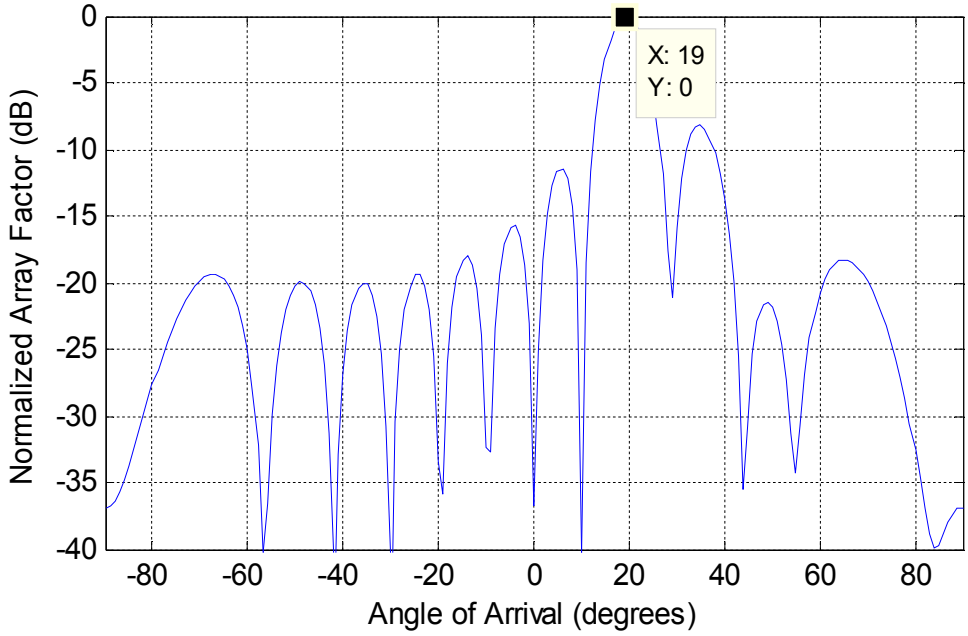
X: 19
Y: 0
Normalized Array Factor (dB)
Angle of Arrival (degrees)
0
-5
-10
-15
-20
-25
-30
-35
-40
-80
-60
-40
-20
0
20
40
60
80

(a)

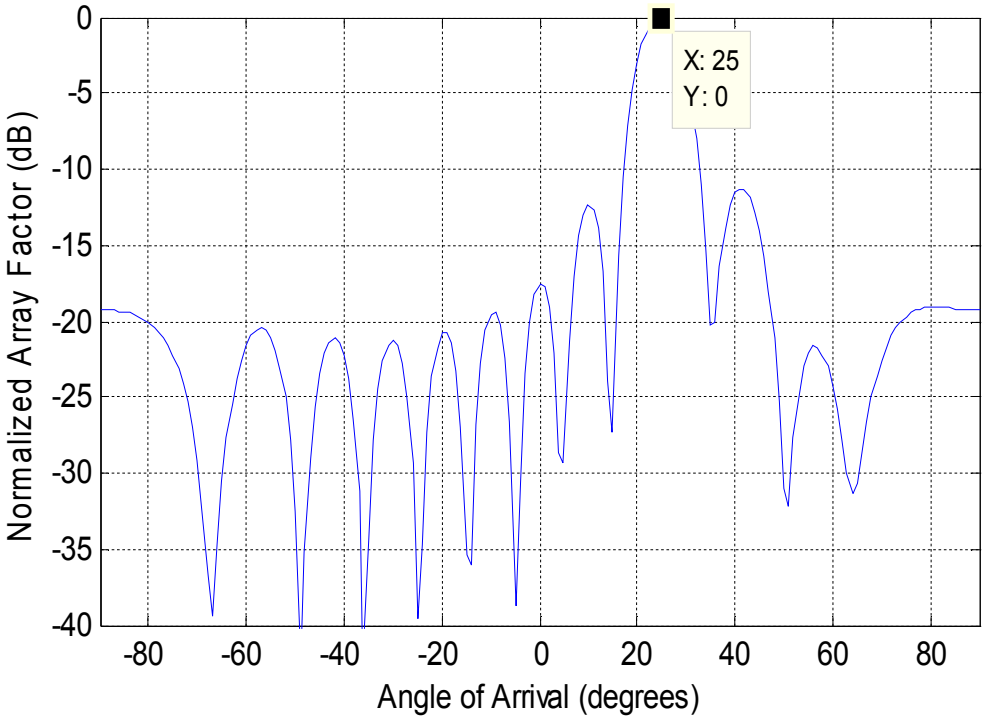
X: 25
Y: 0
Normalized Array Factor (dB)
Angle of Arrival (degrees)
0
-5
-10
-15
-20
-25
-30
-35
-40
-80
-60
-40
-20
0
20
40
60
80

(b)

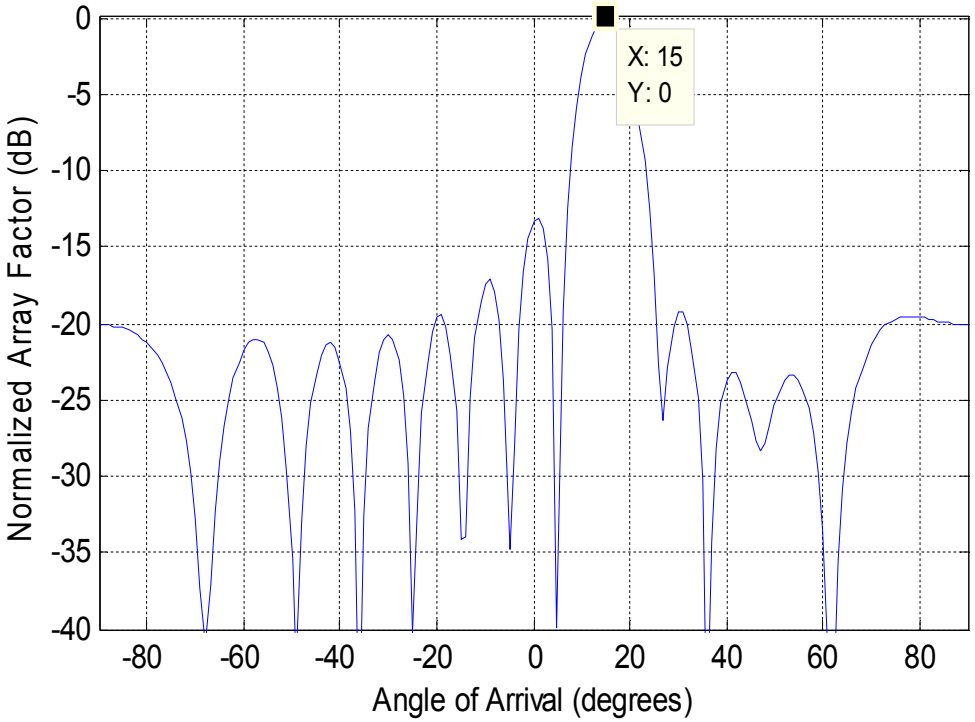

(c)

Figure 6.6, Array factor verses Angle of Arrival for (a) the first signal group (b) the second signal group (c) the third signal group using NLMS algorithm

6.2 Some Factors Affecting Beamformation

Some of the factors affecting the beamformation in adaptive beamforming include, number of array elements and element spacing. The effects of these two parameters are discussed in this section.

6.2.1 Effect of number of array elements on beamformation

Uniform linear array with element inter spacing of 0.5λ is consider and 500 iterations are performed. The SOI has an AOA at 15^0 and SNOI at 40^0, 60^0 and 30^0. Fig. 6.7 shows this effect on LMS algorithm while Fig. 6.8 shows the effect on NLMS algorithm for 12 and 20 array elements.

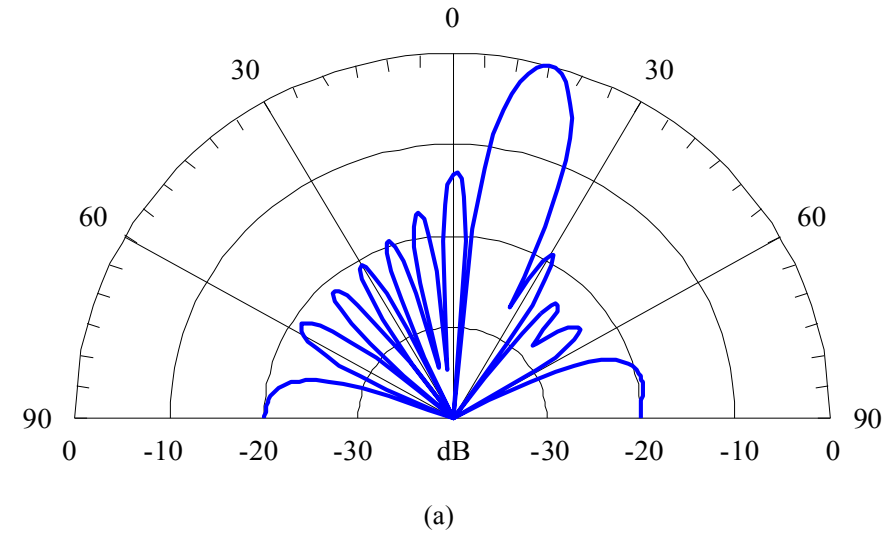

(a)

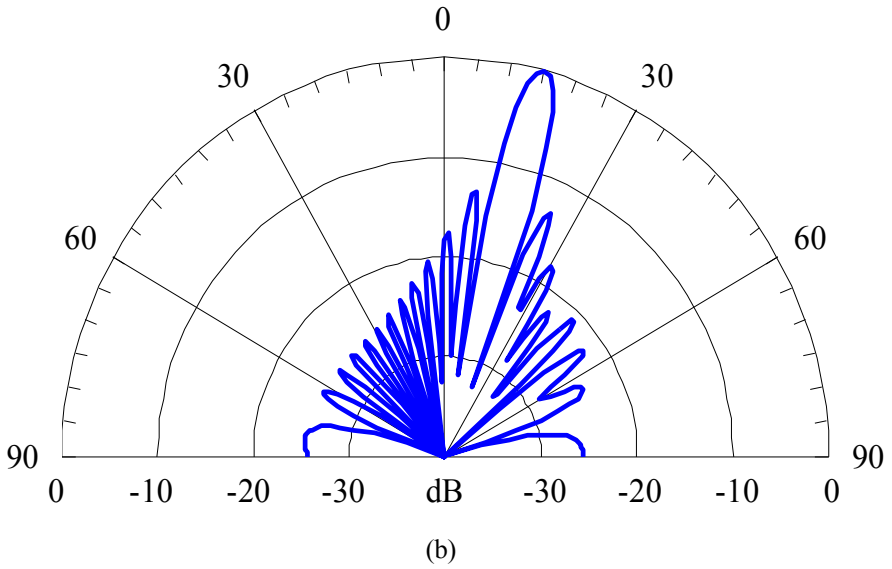

(b)

Fig. 6.7: Impact of number of number of elements on radiation pattern for (a) M=12, (b) M=20, using LMS algorithm.

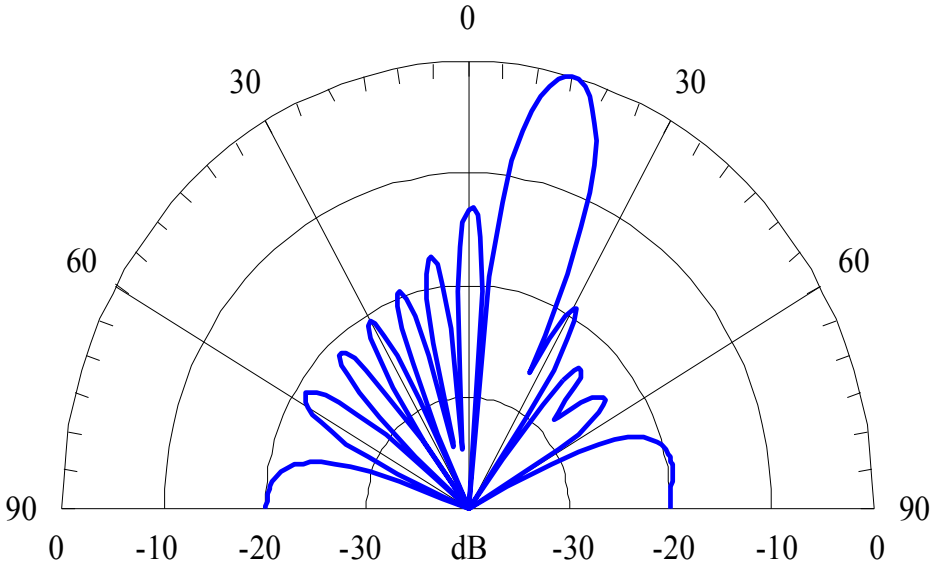

(a)

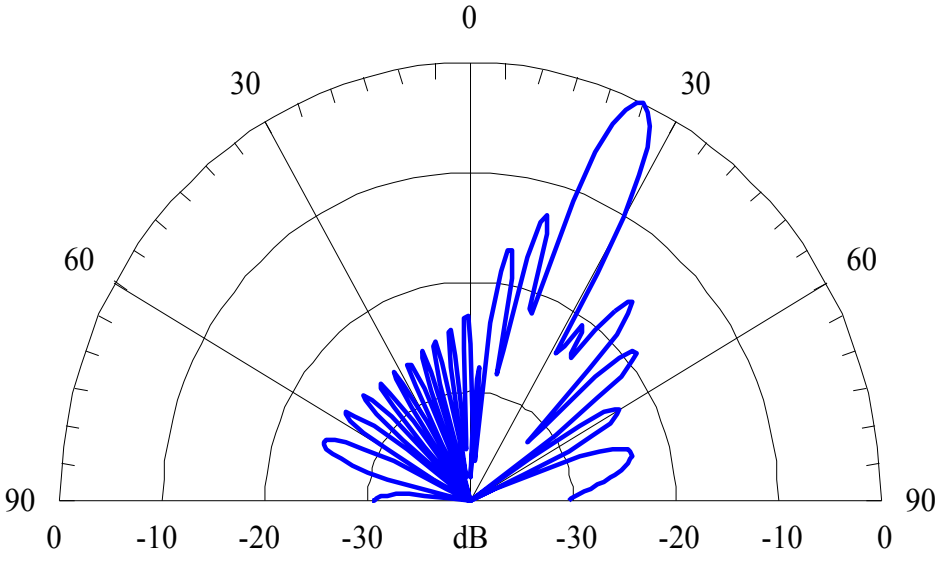

(b)

Fig. 6.8: Impact of number of number of elements on radiation pattern for (a) M=12, (b) M=20, using NLMS algorithm.

The following observation can be made with regard to Fig. 6.7 and 6.8.

The width of the main lobe decreases as the number of array elements is increased; in other words, it becomes narrower. This is crucial for the applications of smart antennas when a single narrow beam is required to track a mobile or cluster of mobiles.

The number of sidelobes increases. In addition, the level of the first and subsequent sidelobes decreases compared with the main lobe. Sidelobes represent power radiated or received in potentially unwanted directions. So in a wireless communications system, sidelobes will contribute to the level of interference spread in the cell or sector by a transmitter as well as the level of interference seen by a receiver when antenna arrays are used.

The number of nulls in the pattern increases. In interference cancellation applications, the directions of these nulls as well as the null depths have to be optimized.

6.2.2 Effect of elements inter-spacing on beam formation

The element inter-spacing *d* also has a significant impact on the shape of the radiation pattern. The simulation carried out with this regard considers 500 iterations for 12 array elements. The spacing between elements is increased from 0.5λ to λ in Fig. 6.9 and Fig. 6.10 for both LMS and NLMS respectively.

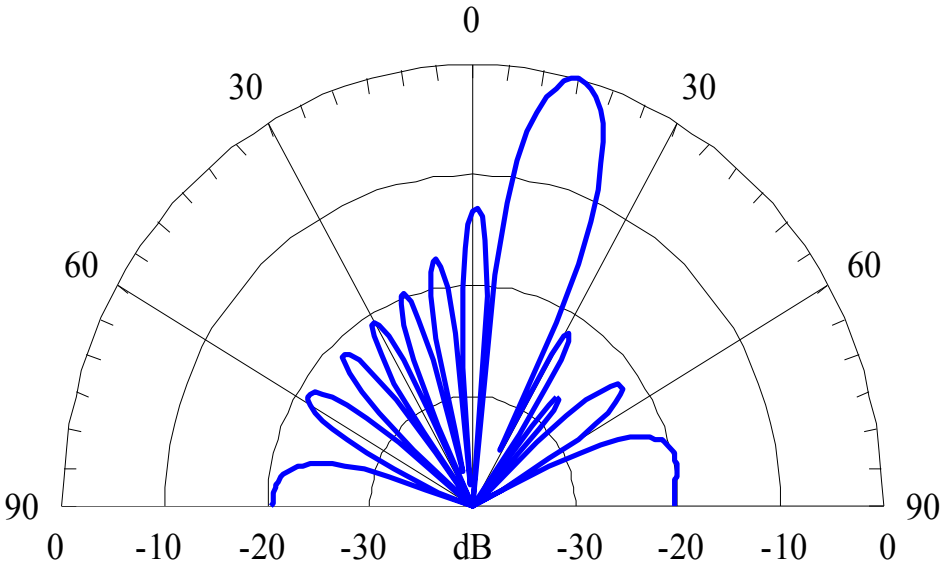

(a)

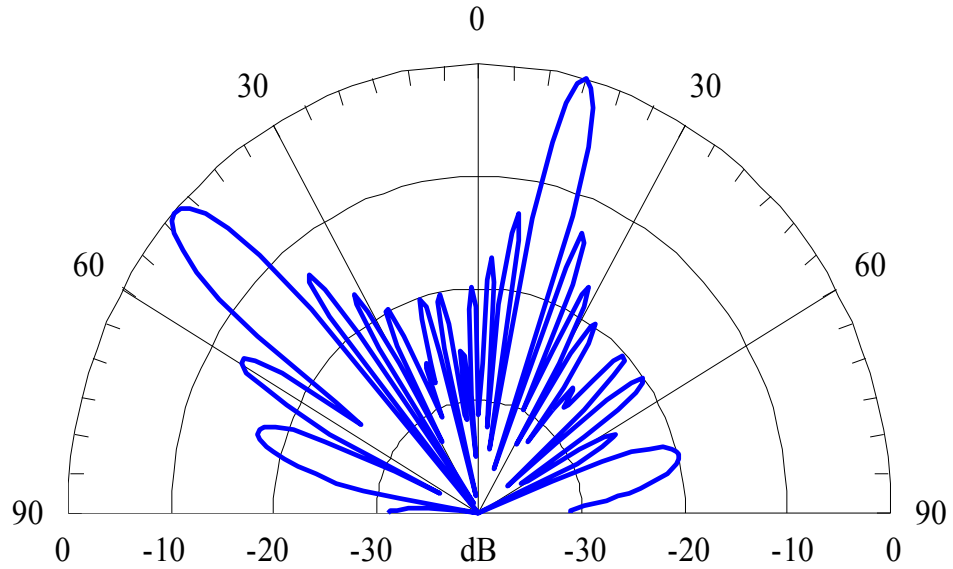

(b)

Fig. 6.9: Impact of element spacing on radiation pattern for (a) d=0.5λ and (b) d=λ, using LMS algorithm.

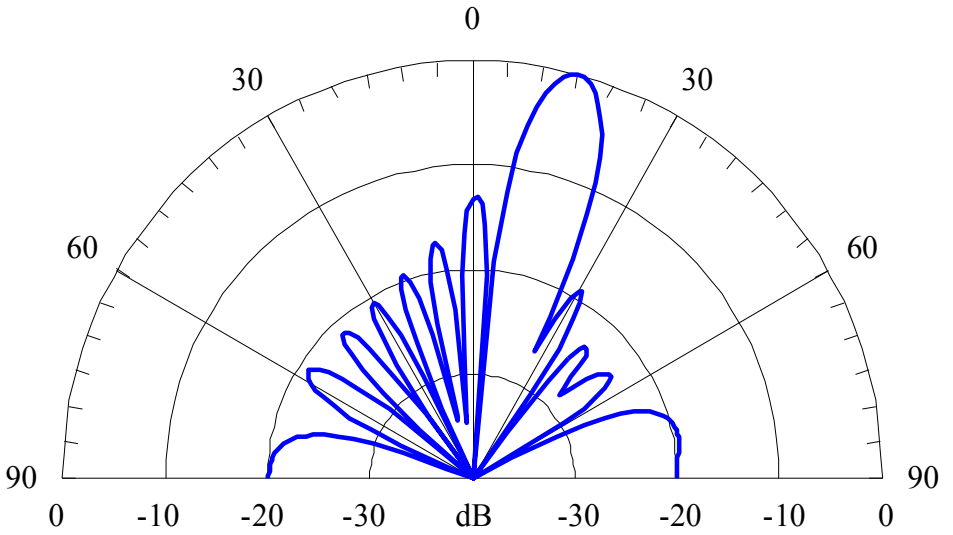

(a)

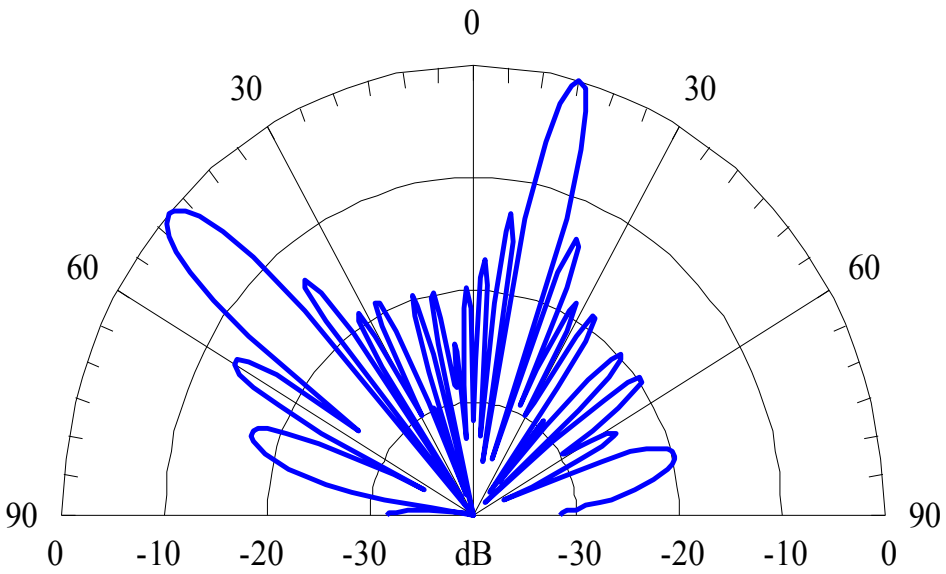

(b)

Fig. 6.10: Impact of element spacing on radiation pattern for (a) d=0.5λ and (b) d=λ, using NLMS algorithm.

Figure 6.9 (a) and 6.10 (a) show the polar radiation pattern of a broadside 12-elementarray with element spacing of d = λ/2. It can be seen that for this element separation, aside from a few sidelobes, there is one main lobe directed toward 15° in each case. When the spacing is increased to d = λ, the radiation patterns become as shown in Fig. 6.9 (b) and 6.10 (b) for LMS and NLMS respectively. The appearance of the grating lobe in the Figures not only have wasted power but also caused more interference to the mainlobe. In practice, the optimum element spacing for beamforming and adaptive interference cancellation applications is d = λ/2.

6.3 Comparison of Steepest Descent, LMS and Normalized LMS in terms of Signal Power Reduction and Computation Time

The table 6.1 and 6.2 respectively gives the comparison of steepest descent (SD), least mean square (LMS) and normalized LMS algorithms in terms of power level reduction and run time for the case M=12 and Np=500.

Table 6.1: Comparison of Steepest descent, LMS and NLMS algorithms in terms of Signal Power Reduction (dB).

Group	First Group			Second Group			Third Group		
Trial	1st trial	2nd trial	3rd trial	1st trial	2nd trial	3rd trial	1st trial	2nd trial	3rd trial
S D	5.64	5.80	5.25	5.12	5.27	5.57	1.71	2.01	3.16
LMS	0.53	0.85	0.98	0.34	0.30	0.35	0.64	1.03	1.01
NLMS	1.79	2.86	1.52	0.82	1.12	1.75	1.99	1.85	1.60

It can be seen from table 6.1 that, LMS has minimum power reduction in each trial with 1.03 dB at most. Steepest descent has much power reduction of at least 1.71dB and maximum of 5.8 dB while NLMS has maximum and minimum power reduction of 1.79 dB and 0.82 dB respectively.

Table 6.2: Comparison of Steepest descent, LMS and NLMS algorithms in terms of computation time (sec)

Group	First Group			Second Group			Third Group		
Trial	1st trial	2nd trial	3rd trial	1st trial	2nd trial	3rd trial	1st trial	2nd trial	3rd trial
S D	4.18	4.05	3.96	3.96	4.00	3.98	4.13	3.99	3.97
LMS	3.25	3.05	3.26	3.12	3.27	3.35	3.10	3.17	3.42
NLMS	2.93	2.99	2.97	2.98	3.03	3.06	3.06	3.07	3.00

The steepest descent method as can be seen from table 6.2 took the longest time to perform the required task in all the trials, followed by least mean square method and NLMS has least run time among the three algorithms compared.

7. CONCLUSIONS and FUTURE WORK

7.1 Conclusions

In this thesis, the implementation of smart antenna system for unknown non-coherent source groups containing coherent signals is carried out in MATLAB. The combination of JADE/high-resolution DOA algorithms are realized to estimate the direction of arrivals (DOA) of the incident signals on the antenna elements. Here, MDL criterion is used to determine the number of noncoherent source groups under white Gaussian noise, JADE algorithm is utilized to estimate the steering vectors. Then, DOA algorithm such as MUSIC, Min-norm, root-MUSIC, ESPRIT and MFBLP used in this thesis is applied to each steering vectors to estimate DOAs. The concept of correct matching between the multiple frequencies and noncoherent source groups is also developed in this study. In order to evaluate the performances of proposed combined algorithm along with new frequency matching approach and also compare the numerical results with different well-known DOA algorithms, several simulations are run in a challenging environment having severe multipath effects with very high fading coefficients and close arrival angles. The simulations are carried out to show the performances of the above mentioned algorithms in the step of DOA estimation after JADE process. The sensitivities of the algorithms to several parameters (SNR, number of antenna elements, snapshots) and the effects of these parameters on the results are also examined. The results show that MFBLP algorithm combined with JADE gives better performance at almost all different scenarios. It is observed that MFBLP has calculated RMSE values below 0.5 degrees for the different parameter conditions of either SNR = 0 dB or antenna element number of 10 or number of snapshot of 500. Besides, the simulations also show the effectiveness of the proposed frequency matching approach, which brings 100 percent accuracy rate of the “correct” matching for MFBLP and ESPRIT algorithms even at the low SNR level of 0 dB.

The DOAs obtained by the JADE-MFBLP algorithm are processed using Steepest Descent, LMS and NLMS adaptive beamforming algorithms. Although all the three methods have successfully steered mainlobes of the adaptive beamforming patterns to the signal of interest and the nulls to the signals not of interest in each non coherent group, steepest descent method has poor resolution and produced several sidelobes with high amplitude. The signal power reduction of 1.04 dB, 2.86 dB and 5.80 dB for LMS, NLMS and steepest descent respectively, are observed at M=12 and snapshots, Np=500.

As a conclusion, the algorithm as the combination of JADE and MFBLP attached with the developed frequency matching and LMS beamforming algorithm has been decided to be reasonable choice for the smart antenna application in the presence of unknown number of noncoherent source groups consisting of coherent signals.

7.2 Future Work

The entire study contains only simulation results of smart antenna implementation for unknown non-coherent source groups containing coherent signals. It is recommended here that the hardware be produced to actualize the study.

Also the number of coherent signals in each group is assumed to be known unlike the number of non-coherent source groups. Therefore, it is suggested that this number be regarded as unknown and determined using well known signal detection algorithms such as minimum description length (MDL) and Akaike Information Theoretic Criterion (AIC) and so on, in future work.

BIBLIOGRAPHY

Balanis C. A., 2005, *Antenna Theory: Analysis and Design*, 3rd edition, John Wiley & Sons, Inc., New York

Barabell A. J., 1983, "Improving the Resolution Performance of Eigenstructure-based Direction Finding Algorithms," in *Proceedings of the IEEE International Conference on Acoustics, Speech and Signal Processing,* pp. 336–339

Cardoso J. F. and Souloumac A., 1993, "Blind Beamforming for Non-Gaussian Signals," IEEE Proceedings-F, vol. 140, pp. 362-370

Chen Z. and Gokeda G., and Yu Y., 2010, Introduction to Direction-of-Arrival Estimation, Artech House, Boston, London

Cheng Qi, 2005, "Choice of Root in Root-MUSIC for OFDM Carrier Frequency Offset Estimation," 2005 Asia-Pacific Conference on Communications, Perth, Western Australia, pp. 534-536

Hayes M. H., 1996, *Statistical Digital Signal Processing and Modelling,* John Wiley & Sons, Inc., New York

Haykin S, 1991, *Adaptive Filter Theory, 2nd Edition*. Prentice-Hall Inc., New Jersey

Jain R.K, Katiyar S. and Agrawal N.K, 2011, ''Smart Antenna for Cellular Mobile Communication,'' VSRD-International Journal of Electrical, Electronics & Communication Engineering, Vol. 1 (9), pp. 530-541

Kawitar R. and Wakde D. G., 2005, "Advances in Smart Antenna System", Journal of Scientific & Industrial Research, vol. 64, pp. 660-665

Khan, Z.I., Awang, R.A. Sulaiman, A.A. Jusoh, M.H. Baba, N.H. Kamal, M.M.D. and Khan, N.I., 2008, "Performance analysis for Estimation of signal Parameters via Rotational Invariance Technique (ESPRIT) in estimating Direction of Arrival for linear array antenna", IEEE International Conference on RF and Microwave Conference, pp530 – 533

BIBLIOGRAPHY (continue)

Khumane D.D., Jadhav A.N. and Bhosale S.D., 2011, ‘‘Dynamic Analysis for Direction of Arrival Estimation and Adaptive Beamforming for Smart Antenna,’’ International Journal of Electronics and Communication Engineering, Volume 4, no.4, pp. 415-423

Kumaresan R. and Tufts D. W., 1983, “Estimating the angles of arrival of multiple plane waves,” *IEEE Transactions on Aerospace and Electronic Systems*, vol. AES-19, pp. 134–138

Moghaddam S. S. and Akbari F., 2012, “Improving LMS/NLMS-based beamforming using Shirvani-Akbari array,” American Journal of Signal Processing, vol. 2, no. 4, pp. 70–75

Nwalozie G.C., Okorogu V.N, Maduadichie S.S, and Adenola A., 2013, ‘‘ A Simple Comparative Evaluation of Adaptive Beam forming Algorithms,’’International Journal of Engineering and Innovative Technology, Volume 2, Issue 7, pp 417-424

Okamoto G.T., 2002, Smart Antennas and Wireless LANS. Kluwer Academic Publishers, Norwell Mass

Pillai S. U., 1989, “Forward/Backward Spatial Smoothing Techniques for Coherent Signal Identification,” IEEE Transactions on Signal Processing, vol. 37, pp. 8-15

Poluri A. and kumar A., 2013, ‘‘Beam steering in Smart Antennas by using Low Complex Adaptive Algorithms,’’Vol. 02 Issue 10, pp. 545-551

Poularikas A.D. and Ramadan Z.M., 2006, *Adaptive Filtering Primer with Matlab*,New York: Taylor & Francis Group

Rao B.D. and Hari K.V.S., 1989, “Performance analysis of ROOTMUSIC,” IEEE Transactions on Acoustics, Speech and Signal Processing, Vol. 37, pp. 1939-1949

BIBLIOGRAPHY (continue)

Roy R., and Kailath T., 1986, "ESPRIT - A Subspace Rotation Approach to Estimation of Parameters of Cissoids in Noise," IEEE Trans. Acoust.,Speech, Signal Processing, vol. 34, pp. 1340-1342

Schmidt R. O., 1986, "Multiple emitter location and signal parameter estimation," *IEEE Transactions on Antennas and Propagation*, vol. AP-34, pp. 276–280

Stevanovi´c I., Skrivervik A., and Mosig J. R., 2003, "Smart antenna systems for mobile communications," Ecole Polytechnique F´ed´erale de Lausanne, Lausanne, Suisse, Tech. Rep

Stoica P. and Moses R., 2005, Spectral Analysis of Signals, Pearson, Upper Saddle River, New Jersey

Stoica P., Ottersten B., Viberg M. and Moses R. L., 1996, "Maximum Likelihood Array Processing for Stochastic Coherent Sources," IEEE Transactions on Signal Processing, vol. 44, pp. 96-105

Tsoulos G.V., Meach M.A., 1995, Swalas S.C. Adaptive Antennas for Third Generation DS-CDMA Cellular Systems, Proceedings of the 45th Vehicular Technology Conference, vol. 1, pp. 45-49

Tsoulos, G.V., 1999, "Smart antennas for mobile communication systems: benefits and challenges," IEEE Electronic & Communication Engineering Journal, vol. 11, no.2 pp. 84-94

Tufts D. W. and Kumaresan R., 1982, "Estimation of frequencies of multiple sinusoids: Making linear prediction perform like maximum likelihood," IEEE Proc., vol. 70, pp. 975-989

Varade S. W., Kulat K.D., 2009 "Robust Algorithms for DOA Estimation and Adaptive Beamforming for Smart Antenna Application," Second International Conference on Emerging Trends in Engineering and Technology, ICETET-09, pp. 1195-1200

BIBLIOGRAPHY (continue)

Wax M. and Kailath T., 1985, "Detection of Signals by Information Theoretic Criteria," IEEE Transactions on Acoustics, Speech and Signal Processing vol. 33, pp. 387- 392

Widrow, B., et.al., 1967, ''Adaptive Antenna Systems,'' *Proceedings of the IEEE,* vol. 55, no. 12, pp. 2143-2159

Yilmazer N., Koh J. And Sarkar T. K., 2006, "Utilization of a Unitary Transform for Efficient Computation in the Matrix Pencil Method to Find the Direction of Arrival," IEEE Transactions on Antennas and Propagation vol. 54, pp. 175- 181

Yuen N and Friedlander B., 1997, DOA Estimation in Multipath: An Approach Using Fourth-15 OrderCumulants. *IEEE Transactions on SignalProcessing*; 45: 1253-1263

Zhang Y., Ye Z. and Xu X., 2008, "Multipath DOA and Fading Coefficients Estimation Using Fourth-Order Cumulants," ICSP 2008 International Conference on Signal Processing, Beijing, pp. 374-377

APPENDIX : A SAMPLE MATLAB CODES FOR DOA ESTIMATION AND FREQUENCY MATCHING USING ESPRIT ALGORITHM

```
close all
clear all
N=2000;

% The coefficients of the signals

a(1)=1; a(2)=-0.6426+i*0.7266; a(3)=0.8677+i*0.0632; a(4)=0.7319-
i*0.1639;
a(5)=1; a(6)=-0.8262+i*0.4690; a(7)=0.1897-i*0.8593; a(8)=0.2049-
i*0.7630;
a(9)=1; a(10)=-0.1681-i*0.9045; a(11)=-0.7293-i*0.1750;
a(12)=0.6102+i*0.1565;

%True Angle of arrivals

b(1)=10; b(2)=20; b(3)=28; b(4)=45;
b(5)=5; b(6)=25; b(7)=35; b(8)=55;
b(9)=40; b(10)= 60; b(11)= 15; b(12)= 30;
b=b*pi/180;

%%%%% The formation of received signals X %%%%%%%%%%
% M = Number of Antenna Elements
% N = Number of iterations
% d = Elements spacing
d=0.5;
L=4; G=12;
temp77=0;
temp11=0;
thet=zeros(1,12);
tic
for iter=1:1
    for M=1:12
        temp=0;
        for k=1:L
            temp1=abs(a(k))*exp(j*(2*pi*20e6*(0:N)*1e-
9+angle(a(k)) - 2* (M-1)*pi*d*sin(b(k)) )); %first group of the
%signals
            temp=temp+temp1;
        end
        aef1check=temp;

        temp=0;
        for k=L+1:2*L
            temp1=abs(a(k))*exp(j*(2*pi*25.5e6*(0:N)*1e-
9+angle(a(k)) - 2*(M-1)*pi*d*sin(b(k)))); %second group of the
%signals
            temp=temp+temp1;
        end
        aef2check=temp;

        temp=0;
        for k=G-L+1:G
```

```
            temp1=abs(a(k))*exp(j*(2*pi*32e6*(0:N)*1e-
9+angle(a(k)) - 2* (M-1)*pi*d*sin(b(k))));  %third group of the
%signals
            temp=temp+temp1;
        end
        aef3check=temp;

        X_noiseless(M,:)=aef1check+aef2check+aef3check; %noiseless
%signal

        %%%adding noise with complex awgn (AWGN)
        X(M,:)=awgn(X_noiseless(M,:),10);


    end

    R=(X*X')/(N+1);     % compute spatial coveriance matrix

    [U,D,V]=svd(R);      % compute eigendecomposition of coveriance
%matrix
    e=diag(D);

    for k = 0 : M-1
        la = e(k+1:M);
        lam=la.^(1/(M-k));
        MDL(k+1)= - (M-k)* (N+1) * log10 ( prod (lam)/ (
sum(e(k+1:M)) / (M-k) )  ) +0.5*k*(2*M-k)*log10((N+1)); % source
%detection using MDL

    end

    [min1,index]=min(MDL);
    index_MDL=index-1;


    [A,S]=jade(X-mean(X,2)*ones(1,N+1),index_MDL);  % steering
%vectors estimation using JADE algorithm

    % Estimate DOAs using Esprit algorithm
        m=M/2;

    w2=[1 0 0 0];
    for column=1:index_MDL
        y=A(:,column);
        R3=zeros(m,m);

        for ii = m : M,
            R3=R3+y(ii:-1:ii-m+1)*y(ii:-1:ii-m+1)'/N;
        end


        % get the eigendecomposition of R3; use svd because it
%sorts eigenvalues
        [U4,D4,V4]=svd(R3);
        S1=U4(:,1:4);

        phi1 = S1(1:m-1,:)\S1(2:m,:);
        abs(eig(phi1));
```

```
        w1=angle(eig(phi1));
        doa1(:,column)=(asin(w1/d/pi/2)*180/pi);

        % Fading coefficient estimation

        A_fading=exp(-j*pi*(0:(M-1))'*sind(doa1(:,column))');

        rho_k1=pinv(A_fading)*y/(w2*pinv(A_fading)*y);
        [max1,index2]=max(rho_k1);
        rho_k(:,column)=rho_k1/rho_k1(index2);

    end
    rho_k;
    rho_k2(:,iter)=rho_k(:);
    doa1;
doa2(:,iter)=doa1(:);

    % compute root mean square error(RMSE) for fading coefficients

    for kk=1:12
        [min7,index7]=min(abs(rho_k(kk)-a(:)));
        thet(index7)=thet(index7)+rho_k(kk);
        temp77=temp77+(min7)^2;



    end

    % compute root mean square error (RMSE)for DOAs
    for kk=1:12
        [min3,index5]=min(abs(doa1(kk)-b(:)*180/pi));
        thet(index5)=thet(index5)+doa1(kk);
        temp11=temp11+min3^2;

    end


    % Frequency estimation part
    N2=500;
    for kl=1:M
        y51=X(kl,1:N2).';
        N1=length(y51);
        m6=200;
        n=index_MDL;
        % compute the sample covariance matrix
        R56=zeros(m6,m6);
        for ii = m6 : N1,
            R56=R56+y51(ii:-1:ii-m6+1)*y51(ii:-1:ii-m6+1)'/N1;
        end



        % get the eigendecomposition of R;
        [U56,D56,V56]=svd(R56);
        S56=U56(:,1:n);

        phi = S56(1:m6-1,:)\S56(2:m6,:);

        w=sort(-angle(eig(phi)));
```

```
        freq=w*1e9/(2*pi)';

        asdf=exp(j.*(0:N2-1)'*w');
        match=(pinv(asdf)*X(kl,1:N2).');

        match_full(:,kl)=match;

        if kl==1
            match1=match;
        end
        X1(:,kl)=match(1)*exp(j*w(1)*(0:N2-1));
        X2(:,kl)=match(2)*exp(j*w(2)*(0:N2-1));
        X3(:,kl)=match(3)*exp(j*w(3)*(0:N2-1));
    end


    % Frequency (Group) Matching


    mer(1,:)=((exp(j.*- 2.* (0:M-
1)'*(pi.*d.*sind(doa1(:,1))')))*rho_k(:,1)).';
    mer(2,:)=((exp(j.*- 2.* (0:M-
1)'*(pi.*d.*sind(doa1(:,2))')))*rho_k(:,2)).';
    mer(3,:)=((exp(j.*- 2.* (0:M-
1)'*(pi.*d.*sind(doa1(:,3))')))*rho_k(:,3)).';
    table=0;
    for uu=1:3  %%% frequency
        for vv=1:3  %%%% group
            table(uu,vv)=norm(match_full(uu,:)-mer(vv,:));
        end

    end
    table;
    [asdf,col_index]=min(min(table));
    [asdf,row_index(col_index)]=min(min(table'));
    table(:,col_index)=1000;table(row_index(col_index),:)=1000;

    [asdf,col_index]=min(min(table));
    %vdgfdgd
    [asdf,row_index(col_index)]=min(min(table'));
    table(:,col_index)=1000;table(row_index(col_index),:)=1000;

    [asdf,col_index]=min(min(table));
    [asdf,row_index(col_index)]=min(min(table'));




    for kkk=1:index_MDL

        hhh(kkk,iter)= norm(sort(b(4*(row_index(kkk)-
1)+1:4*row_index(kkk))*180/pi)-(sort(doa1(:,kkk)')))/sqrt(4);

    end

end
```

```
doa1;
rho_k;


% std with real doas


z=0;
for kk=1:12
z=z+abs((rho_k(kk)))^2;

end

sd_error77=sqrt(temp77/(iter*(z)));  %RMSE for fading coefficients

sd_error=sqrt(temp11/(iter*12));   %RMSE for DOAs with real values

%std with mean values
me=thet/iter;
temp123=0;
for iter1=1:iter
    for kk=1:12
        [min123,index1]=min(abs(doa2(kk,iter1)-me(:)));

        temp123=temp123+min123^2;
    end
end

sd_error1=sqrt(temp123/(iter*12)); %RMSE for DOAs with mean values

% Number of correct frequency matching
number_correct_matching=length(find(hhh<5))*100/(iter*index_MDL);


toc
```